STUDY ON THE CYCLONE

KOICHI IINOYA

Department of Chemical Engineering

(Received September 30, 1953)

CONTENTS

Introduction

The centrifugal, or cyclone, dust collector is a simple device widely used for separation of solid from fluid. It opposes centrifugal force collinearly to fluid drag, substantially at right angles to a rapid carrying current. The typical cyclone is a cylindro-conical chamber set with axis vertical and apex down. The flow of fluid in a cyclone is complex, and the author traced it by special Pitot-tube measurements. Then he made clear the pressure drop and the collection efficiency theoretically and fundamentally on various kinds of cyclones.

Many other investigators have studied only on a few types of cyclones, and general conclusion has not yet been obtained about the theory and the experimental results.

Chapter I. Spiral Flow in Cylinder

1. PRELIMINARIES

Uniform spiral flow in a central exit pipe and jet spiral flow which is blown tangentially into one-end-opened cylinder from one direction are fundamental flows in a cyclone dust collector. The author measured them with cylindrical (with 3 holes) or spherical (with 5 holes) Pitot tubes.

The uniform spiral flows of water in a draft tube of water turbine have also been researched by others,[1)2)] but the fundamental spiral flows of air have not been measured.

2. EXPERIMENTAL APPARATUS AND METHOD

The experimental apparatus is shown in Fig. 1. 1. Air was sent to a 2″ measuring orifice through a regulation valve from a blower, and was blown tangentially into a closed end of an iron cylinder, the other end of which was open. The cylinder

was 182 mm in diameter and 540 mm in length. The holes for measuring air pressure and velocity were made on the cross section of the cylinder through the inlet center line, and on the two sections which were respectively 250 mm and 450 mm lower than the inlet section. The holes were distributed at 6 equiangular positions on the periphery of each section, and their diameters were 2 mm ϕ for measuring pressure only and 3/8″ϕ for the Pitot tubes.

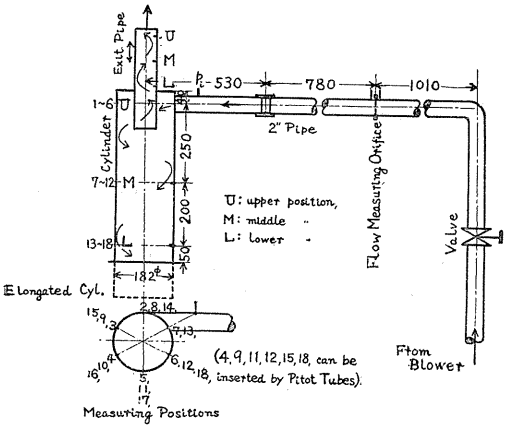

FIG. 1.1. Experimental apparatus.

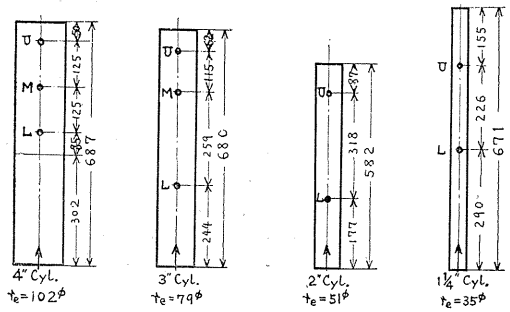

FIG. 1.2. Experimental cylinders of spiral flows.
(U: Upper position. M: Middle position. L: Lower position.)

The cylinder could be elongated to an arbitrary length, and then spiral jet flows in the cylinder were measured.

Moreover uniform spiral flows were examined experimentally in four central exit pipes, when the bottom of the outer cylinder was closed. Measuring points of these exit pipes are also shown in Fig. 1.2.

The diameters of cylindrical Pitot-tubes (with 3 holes) were 4 mm ϕ or 8 mm ϕ, and those of spherical Pitot-tubes (with 5 holes) were 5 mm ϕ (Photo. 1.1).

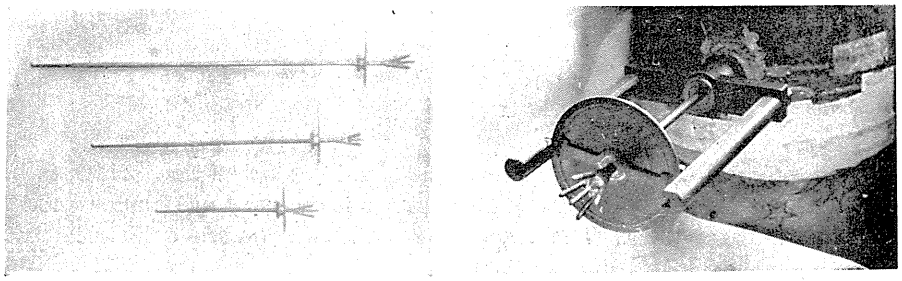

PHOTO. 1.1. Spherical pitot tubes with 5 measuring holes (D=5 mmϕ).

Inlet velocity of air flow was about between 1 m/s and 20 m/s. Measuring errors of spiral flow angles were below 1°, and those of flow velocities were less than 0.5 m/s.

3. EXPERIMENTAL RESULTS

A. Spiral Jet Flow in a Cylinder

The jet flow is diffused, as it goes down spirally. When the cylinder was

elongated to a certain length, the flow condition was suddenly changed. It means that the jet flow was just fully diffused in the cross section of the elongated cylinder end. The change appeared on spiral angle of the flow (Fig. 1.3), pressure (Fig. 1.4) and velocity (Fig. 1.5), *i.e.*, the pressures rised and the spiral angles decreased suddenly.

a. Spiral angles (θ) of the flow were not almost affected by flow quantity except at very small velocities. Radial distributions of the angles are given in Fig. 1.3, and the maximum flow angle was about 40° at the cylinder wall. On the other

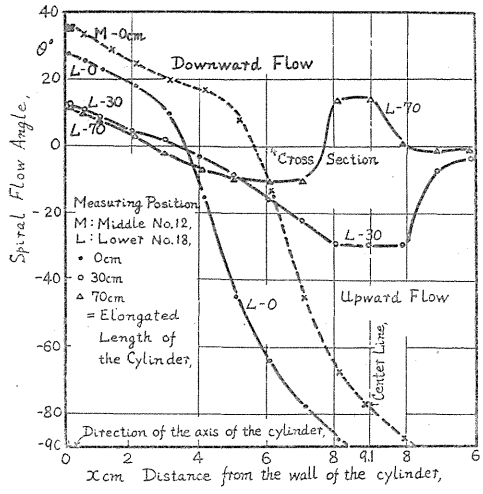

FIG. 1.3. Radial distributions of spiral flow angle θ in a cylinder (Spiral jet flow).

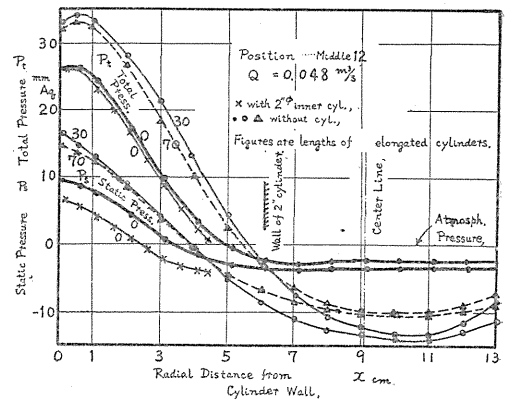

FIG. 1.4. Radial pressure distributions in a cylinder (Spiral jet flow).

hand, radial flow angle β_1 against the tangential direction on the cross section was below about 20°.

b. Velocities were nearly proportional to flow quantities, and pressures were proportional to the square of them, but in small quantities these proportionalities at any points in the cyclone did not hold correctly. Adverse flows and negative pressures often happened in the central zone of the cylinder. The position, at which the tangential velocity became zero, did not usually coincide with the cyclone center on account of the eccentricity of the flow center, and the position of $v_z=0$ was not constant, but depended on the width of inlet pipe. Some examples of radial distributions of velocities and pressures are shown in Fig. 1.4 and 1.5.

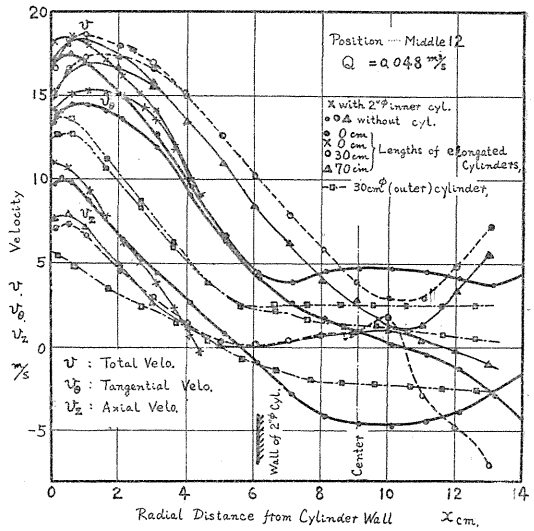

FIG. 1.5. Radial velocity distributions in cylinders (Spiral jet flow).

Circumferential distributions of velocities are also given in Fig. 1. 6, and there are the maximum total and tangential velocities at the zero radial velocity ($v_r=0$). And the jet spiral flow in a cylinder seems to be reflected against its inner wall.

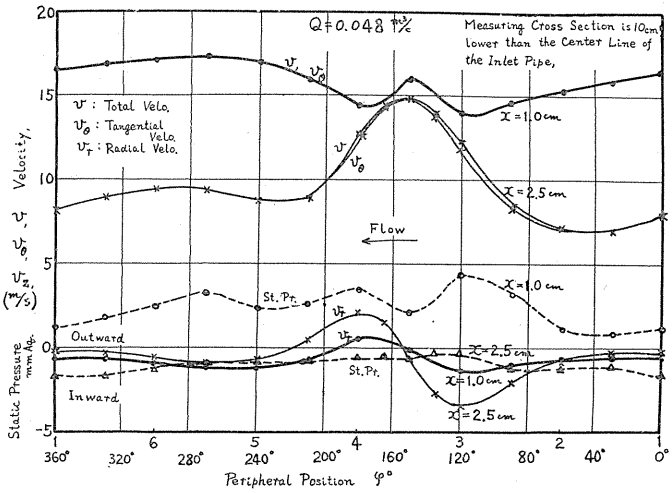

FIG. 1. 6. Peripheral distributions of velocities and static pressures in a cylinder (Spiral jet flow).

B. Uniform Spiral Flow in Cylinders

This flow happens in an exit pipe of a cyclone.

a. Spiral angle θ and velocities v, v_0, v_z, v_r

Radial distributions of spiral angles θ and axial velocities v_z are not constant,

TABLE 1. 1. Positions and Magnitudes of the Max. Velocities. (Uniform Spiral Flows)

Velo. ↓	Cylinder→ / Position ↓	1¼″		2″		3″		4″		Mean radius
		$\frac{v}{V_0}$	$\frac{r}{R}$	$\frac{v}{V_0}$	$\frac{r}{R}$	$\frac{v}{V_0}$	$\frac{r}{R}$	$\frac{v}{V_0}$	$\frac{r}{R}$	$\frac{r_m}{R}$
Max. total velo. $v_{max.}$	U	1.5	0.75	2.0	0.65	2.9	0.60	3.1	0.80	0.7
	M	—	—	—	—	3.2	0.60	3.4	0.55	
	L	1.6	0.70	2.6	0.78	3 4	0.75	3.6	0.70	
Max. tangen. velo. $v_{0max.}$	U	1.1	0.50	1.8	0.45	2.8	0.50	2.9	0.65	0.5
	M	—	—	—	—	3.0	0.50	3.3	0.50	
	L	1.4	0.40	2.2	0.55	3.2	0.55	3.4	0.55	
Max. axial velo. $v_{z\,max.}$	U	1.2	0.80	1.3	0.90	1.6	0.90	1.5	0.90	0.9
	M	—	—	—	—	1.5	0.90	1.6	0.87	
	L	1.2	0.75	1.4	0.90	1.6	0.90	1.8	0.90	
Mean ax. velo.	V_0	10～25		5～15		2～8		1～5		m/s

U: Upper position, M: Middle position,
L: Lower position, r_m: Mean radius at the max. velo.

but decrease inwards. And the spiral angle θ does not depend upon flow quantity and cylinder diameter (Fig. 1.7).

But as the flow goes on forward, the angle θ is increased by the pipe friction. Velocities at any position are almost proportional to the flow quantity, and there is the maximum axial velocity $V_{\theta max.}$ at 90% radius, and axial velocity v_z becomes equal to the mean axial velocity V_0 at 60% radius. There is the maximum tangential velocity $v_{\theta max.}$ at about 50% radius, and the distributions of total and tangential velocities v, v_θ show that there is nearly a forced vortex in the center zone (Fig. 1.8). In Fig. 1.9, the apparent values of radial velocities v_r are comparatively larger on account of the eccentricity of the vortex. An exit pipe with a trumpet-shaped inlet has slightly good characteristics (Table 1.1).

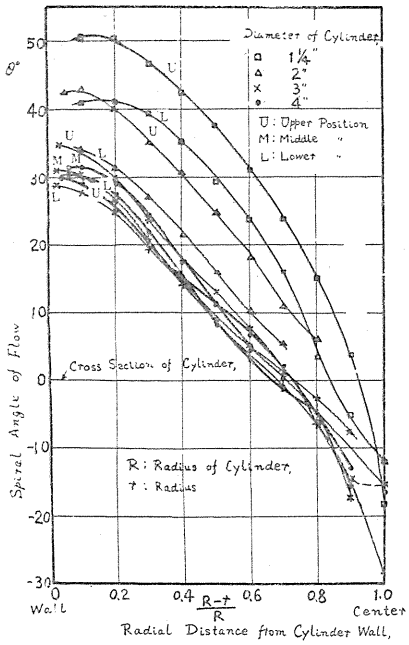

FIG. 1.7. Radial distributions of spiral flow angle in cylinders (Uniform spiral flow).

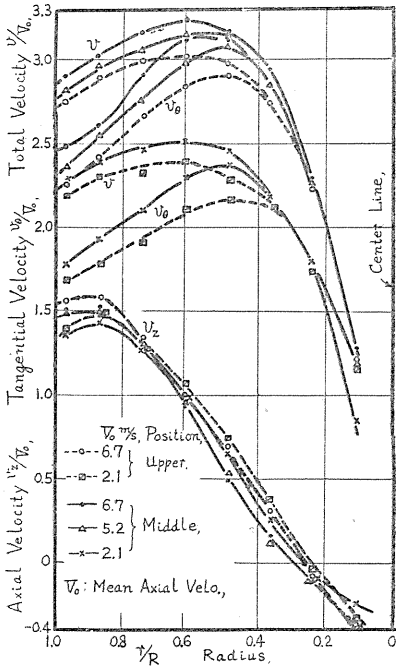

FIG. 1.8. Radial distributions of velocities in a 3″ cylinder (Uniform spiral flow).

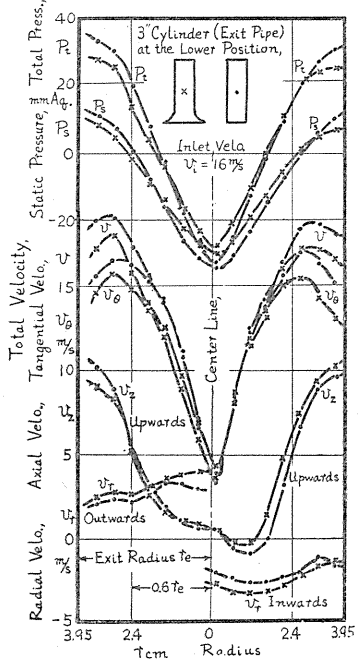

FIG. 1.9. Radial distributions of uniform spiral flow in a 3″ cylinder.

b. Presure

Static pressure is zero at 60% radius in spite of change of flow quantity, and there is negative pressure in the center zone of the cylinder. The value of the maximum total pressure along the wall is nearly equal to the negative value of the minimum one at the center (Fig. 1.9). Radial distribution of static pressures is much the same as the Rankine vortex.

4. Conclusion

Jet and uniform spiral flows were studied with special pitot tubes, and the distributions of flow angles, velocity components and pressures of these flows were measured, and the effects of flow quantities, cylinder diameters, cylinder lengths and inlet forms were shown.

Appendix

On a Solution of Spiral Flows in Cylinders

We use the Navier-Stokes equations of cylindrical co-ordinates[4] and assume the following conditions.

1. Incompressible fluid. ($\rho=$const.)
2. No external forces.
3. Steady state. ($\partial/\partial t=0$)
4. Axial symmetry. ($\partial/\partial\theta=0$)

And when the various conditions below are given, the equations of motion can be solved:

a. When $v_r=0$, and $\partial v_\theta/\partial z=0$,

then, $$v_\theta=Ar+(B/r) \tag{1}$$

$$p/\rho=A^2r^2/2+2AB\ln r-B^2/(2r^2) \tag{2}$$

b. When $\partial v_z/\partial z=0$, and $\partial^2 v_\theta/\partial z^2=0$,

then $$v_\theta=Ar^{1+(c/\nu)}+(B/r) \tag{3}$$

$$v_r\cdot r=c \tag{4}$$

c. When $\partial v_z/\partial z=0$, and $\partial p/\partial z=0$,

then $$v_z=\frac{a\nu}{c}r^{c/\nu}-b \tag{5}$$

$$v_r\cdot r=c \tag{4}$$

d. When $v_r=0$, and $\partial p/\partial z=0$,

then $$v_z=c\log(r/r_1), \tag{6}$$

e. When $v_r=0$, and $\partial p/\partial z=$const.,

then $$v_z=c\log r+br^2+d, \tag{7}$$

f. When $\partial p/\partial z=$const., and $v_r=v_z=0$,

then $$\partial v_\theta/\partial\theta=0$$

$$v_\theta=\frac{1}{2\mu}\frac{\partial p}{\partial\theta}(r\log r)+Br+(C/r),^{5)} \tag{8}$$

g. When $\partial v_z/\partial z=0$, and $\partial p/\partial z=a$ (const.),

then $$v_z=\frac{ar^2}{4\rho(\nu-c/2)}+\text{const.}, \tag{9}$$

Symbols:
v_r : Radial component of velocity,
v_θ : Tangential component of velocity,
v_z : Axial component of velocity,
r : Radius (Radial ordinate),
p : Pressure,
z : Axial ordinate,
ρ : Density,
μ : Viscosity,
ν : Keinematic viscosity $=\mu/\rho$,
A, B, C, a, b, c, d =constant,

Chapter II. Air Flow in Cyclone Dust Collector

1. Preliminaries

The most important factors for the operation of a cyclone dust collector are pressure loss and collection efficiency, and yet we have appreciated only few fundamental and accurate investigations of them. The author measured the air flow in many cyclones by means of special Pitot tubes, and examined the effects of many elements of a cyclone.

2. Experimental Apparatus and Procedures

Experimental apparatus was such in the foregoing chapter. Test cyclones are shown in from Fig. 2.1 to Fig. 2.3, and were made of an iron plate or pipe. No. 1 and No. 2 cyclones had respectively a tangential inlet with a rectangular cross-section. No. 3 cyclone had a tangential inlet with a circular cross-section, and its cone angle could be changed to 15°, 30°, 60° or 180°, and the inner diameter of its exit pipe could also be changed to $1\frac{1}{4}''$, $2''$, $3''$, or $4''$. No. 4 cyclone had a half-spiral inlet with a rectangular cross section (Linden Type),[14] and its exit pipe could be changed, and its conical part could be changed to a bent type, which is called a horizontal cyclone. No. 6 cyclone was a larger one made proportional to No. 4 cyclone. No. 7 cyclone was also of Linden type, and had a small inlet. No. 8 cyclone had a tangential inlet with a rectangular cross-section, and its inlet area and its exit diameter could be changed.

By using three spherical Pitot tubes (short, middle, long) each with five measuring holes and five cylindrical Pitot tubes each with three holes, the author could measure three dimensional flow. They are shown in Photo. 1.1.

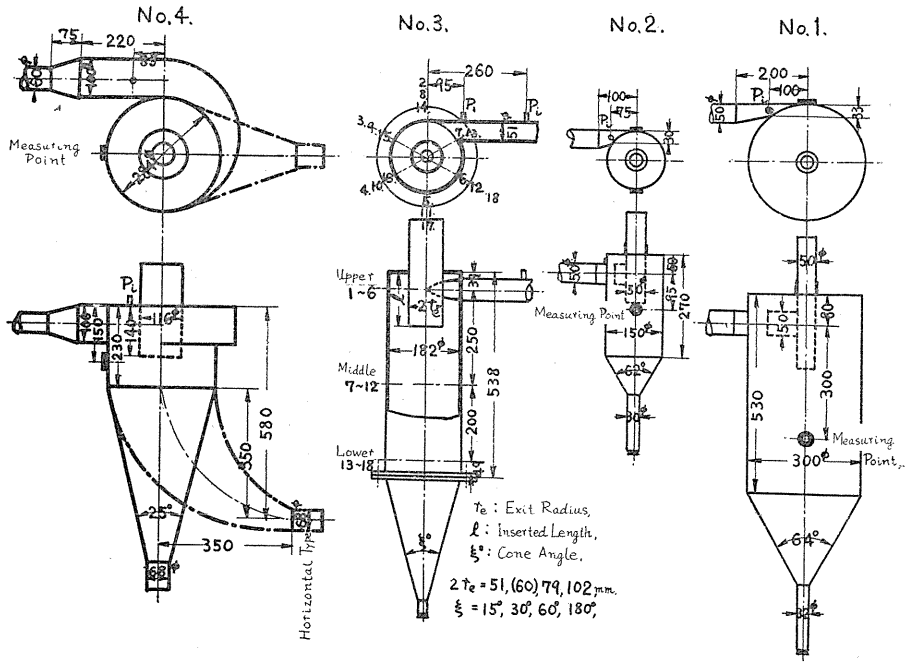

FIG. 2.1. Test cyclones (No. 1, 2, 3, 4).

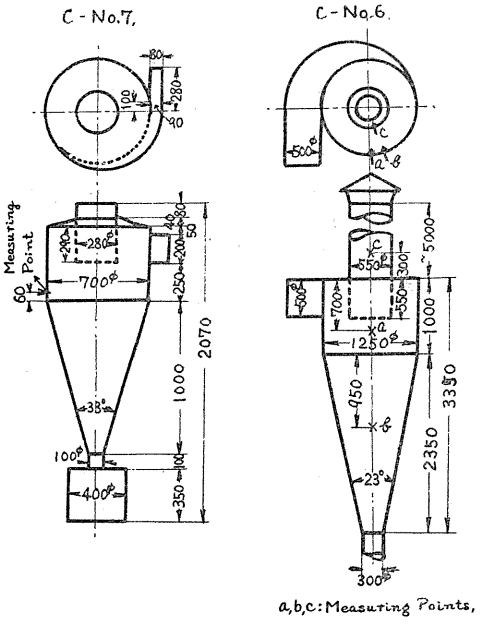

FIG. 2.2. Test cyclones (No. 6, 7).

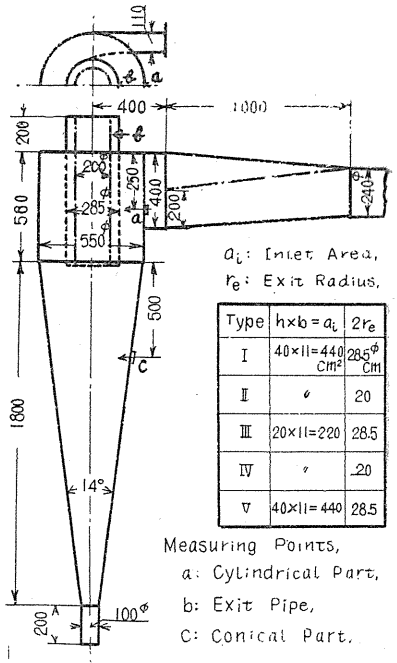

Type	h×b = a_i	$2r_e$
I	40×11=440 cm^2	28.5 cm
II	〃	20
III	20×11=220	28.5
IV	〃	20
V	40×11=440	28.5

Type V has an enlarged guid vane at the inlet.

FIG. 2.3. Test cyclone (No. 8).

3. Experimental Results

1. When air flow quantities are changed in the same cyclone

a. Pressure at any position is almost proportional to the square of flow quantity (Fig. 2.4).

b. Flow angle is nearly constant except at small flow quantities (Fig. 2.5).

c. Flow velocity is almost proportional to flow quantity (Fig. 2.5).

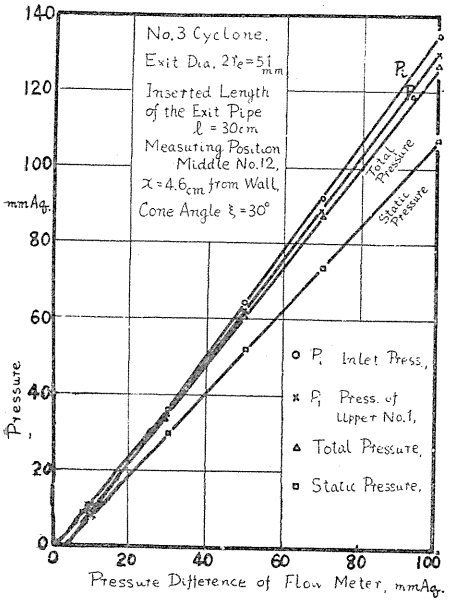

FIG. 2.4. Correlation of pressure and air quantity.

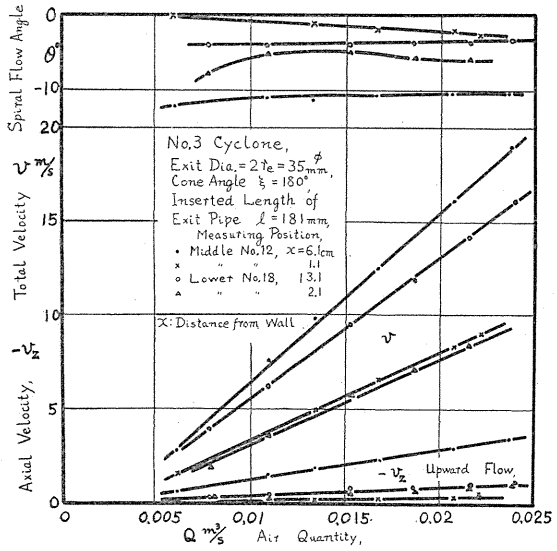

FIG. 2.5. Correlations between air quantity and flow spiral angles or velocities.

2. Measuring Errors of the Pitot Tubes

When the Pitot tube was inserted into a cyclone, the air flow in it changed itself. And its calibration in parallel flow was not strictly applicable to cyclone flow, but the measured results by various Pitot tubes and methods were almost equal to each other, except near the center of the cyclone (Fig. 2.6).

The deeper the Pitot tube was inserted, the lower any pressure and velocity in the cyclone became than true values. Therefore the smallest Pitot tube was desirable (Fig. 2.7).

3. Pressure Distributions. (P_t: Total press., P_s: Static press.)

Axial and circumferential pressure distributions in cyclones are almost constant except near the cyclone inlet. Radial pressure distributions are similar to those of the Rankine vortex. Static pressure at about 60% radius of the exit pipe is generally equal to the exit pressure (atmospheric pressure) in a pressure type cyclone (Fig. 2.8 and 2.8′).

4. Flow Angle Distributions. (θ: Spiral angle, β: Radial flow angle, β_1: Projection of β on the cross section of the cyclone cylinder)

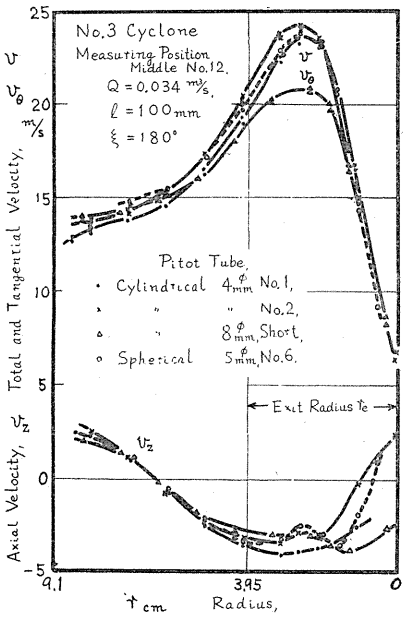

FIG. 2.6. Comparison of four measuring velocity distributions by various Pitot tubes.

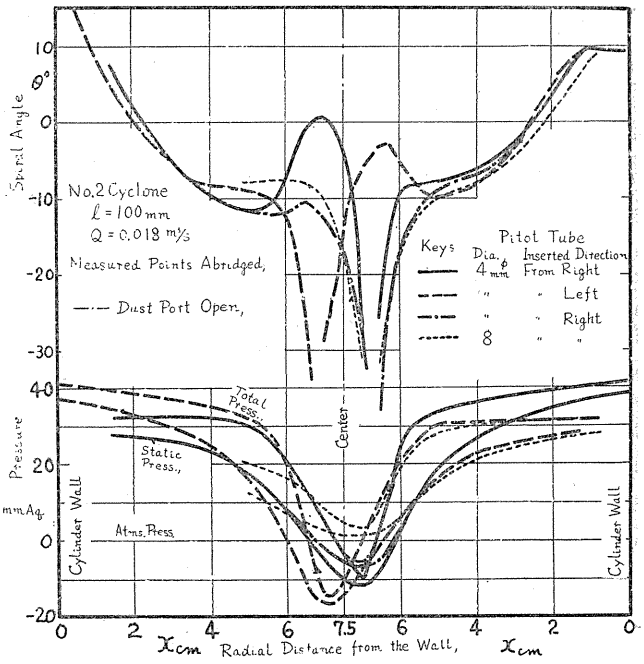

FIG. 2.7. Errors of spiral flow angle and pressure distributions by diameters and inserted lengths of various Pitot tubes.

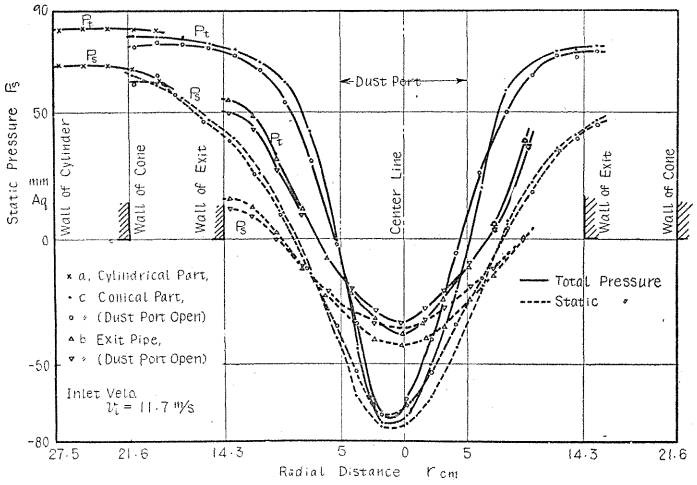

FIG. 2.8. Distributions of total and static pressures (No. 8 Type I Cyclone).

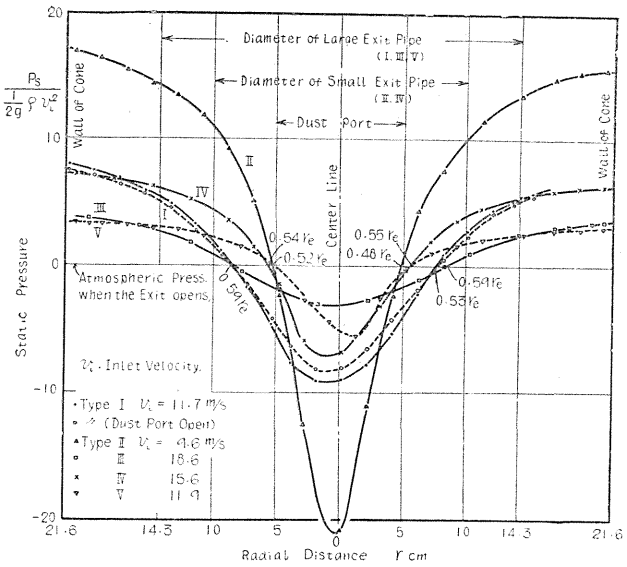

FIG. 2. 8′. Distributions of static pressure (p_s) in various types at the conical part (No. 8 Cyclone).

The distributions of flow angles in a suction type or in a pressure type of low velocity are slightly distinct from the normal ones (Fig. 2. 9).

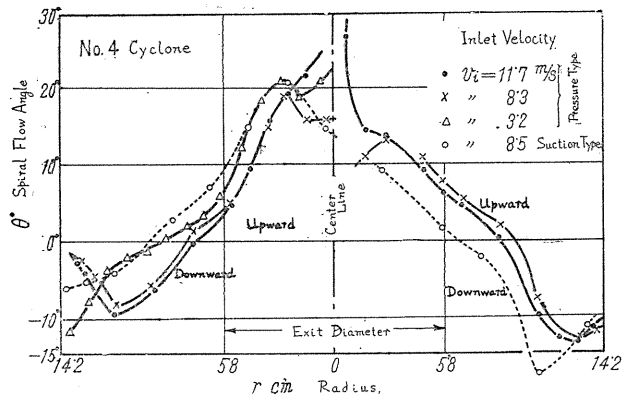

FIG. 2. 9. Radial distributions of spiral flow angles θ at the various conditions (No. 4 Cyclone).

Radial flow angle β is generally small, and spiral angle θ at the concentric part of cylinder is about 7°. These flow angles β, θ are almost independent of the area of inlet or exit pipe.

The angle β cannot be measured with the cylindrical Pitot tube, but the angle β_1 can be measured, when the Pitot is inserted parallel to the cyclone axis. But the angle β can be measured with the spherical Pitot tube, and is almost equal to the angle β_1 in a cyclone.

$$\tan\beta = \tan\beta_1 \cdot \cos\theta$$

generally $\theta < 30°$, then $\beta \fallingdotseq \beta_1$.

5. Velocity Distributions. (v: Total velocity, v_θ: Tangential velocity, v_z: Axial velocity, v_r: Radial velocity)

$$v \sin\beta = v_r, \quad v \cos\beta \cdot \cos\theta = v_\theta, \quad v \cos\beta \cdot \sin\theta = v_z.$$

A. Circumferential Distributions

The total velocities v and the tangential velocities v_θ are nearly constant at any point of the same circumference, where the radial velocities v_r (also β) are

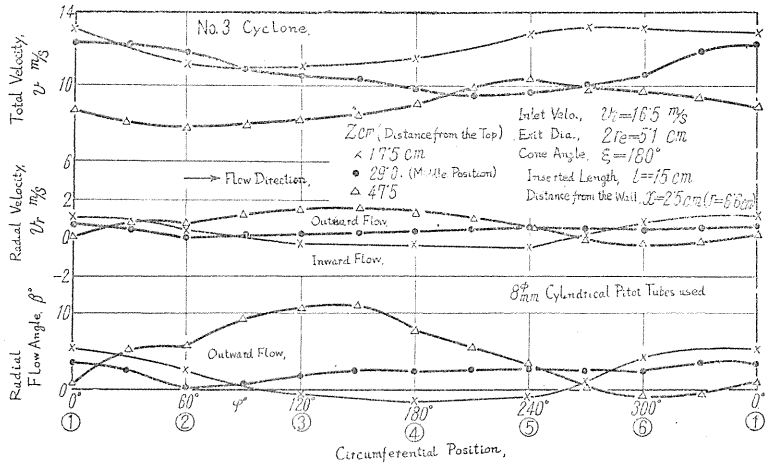

FIG. 2.10. Circumferential distributions of velocities and radial flow angles.

not constant at all, and have often possitive or negative sign there. It means that there is an eccentricity of the flow center (Fig. 2.10). Fig. 2.11 shows three radial distributions of v and v_z at the same cross section of a cyclone, and these distributions are nearly the same in each other.

B. Axial Distributions

Total velocity v and tangential velocity v_θ decrease axially downwards, and are small near the

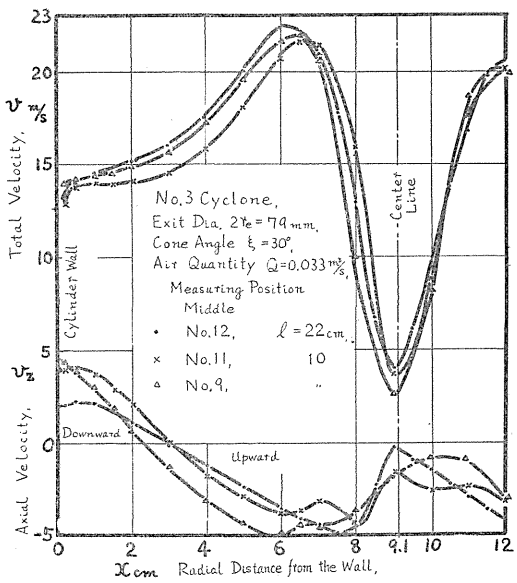

FIG. 2.11. Comparison of three radial distributions of velocities at the same cross section.

outside wall of an exit pipe. Radial velocity v_r shows inward direction at the bottom of a cyclone (Fig. 2.12).

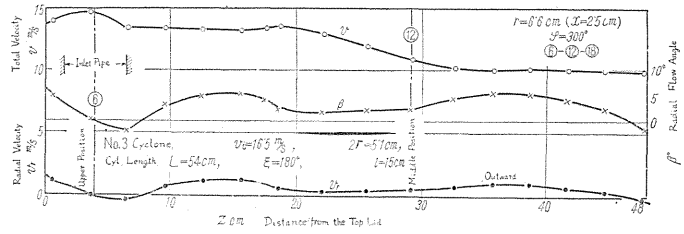

FIG. 2.12. Axial distributions of velocities and radial flow angles.

C. Radial Distributions

The distributions of tangential velocities v_θ show forced vortices inside about 60% radius of exit pipe, and approximate free vortices in the outside. Therefore there is the maximum tangential velocity $v_{\theta max.}$ at about 60% radius of exit pipe.

Axial velocities v_z are generally directed downward at the outer radius, and upward near the center. But the secondary flow appears near the wall of a cyclone. Axial velocity v_z and spiral angle θ change suddenly at the inlet of an exit pipe.

Radial velocity components v_r are small compared with the other components, and have not large variations on the whole.

The centers of the spiral flows do not generally coincide with the cyclone centers (Fig. 2.13).

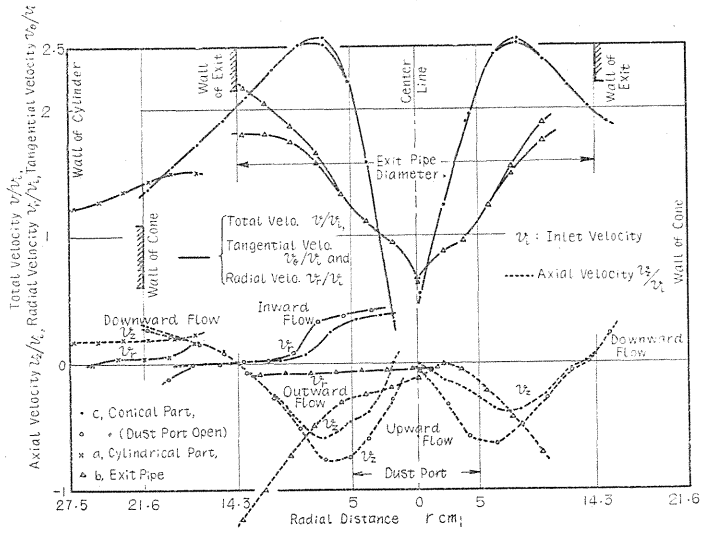

FIG. 2.13. Radial distributions of flow velocities, v, v_θ, v_z, v_r (No. 8-I Cyclone).

a. Effects of cone angle ξ (Fig. 2.14)

When the cone angle ξ becomes smaller, the maximum flow velocity near the center and pressure drop of the cyclone decrease, but the velocity near the cyclone wall

does not change, because only the flow velocity of inner vortex decreases proportionally to the frictional area of the cone.

But the axial velocity component v_z is hardly changed by the cone angle.

b. Effects of exit radius r_e (Fig. 2.15)

In the same air flow, the larger the exit radius grows, the smaller the maximum velocity and pressure drop in the cyclone become. But the peripheral velocity has scarcely any change, and the maximum velocity

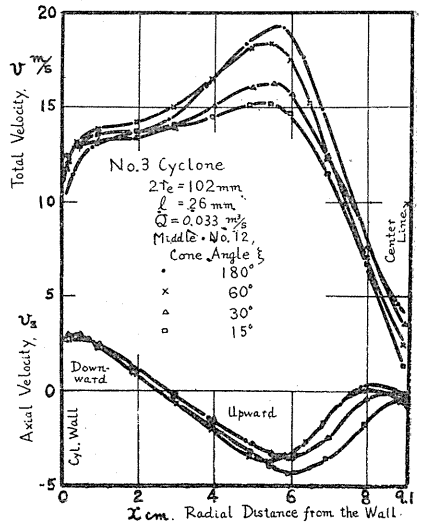

FIG. 2.14. Effects of cone angle on radial distributions of velocities.

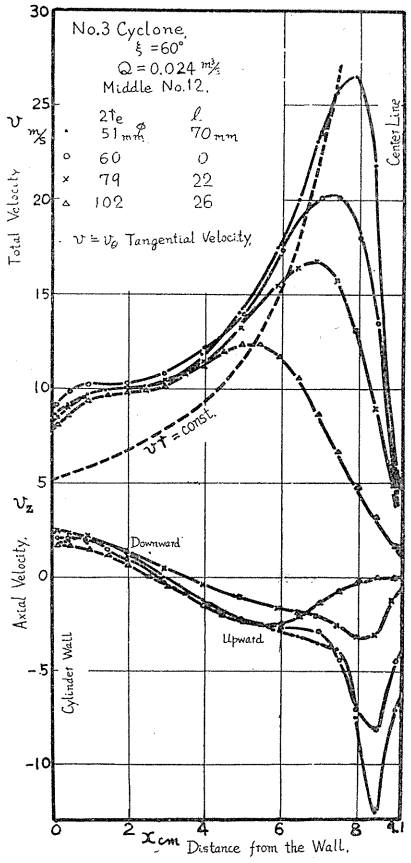

FIG. 2.15. Effects of exit radius on radial distributions of velocities.

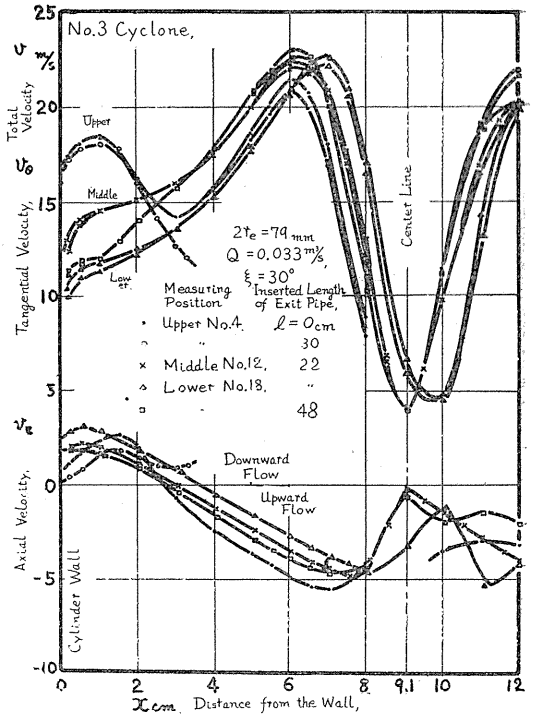

FIG. 2.16. Variations of velocity distributions by the measuring positions.

$v_{max.}$ exists always at 60% radius of the exit pipe. Axial velocity v_z is not quite changed by the exit radius, except in the center zone.

c. Variations by the upper and lower positions

The velocity near a cyclone inlet is equal to the velocity in the inlet pipe on the whole, but at the lower position the velocity dereases by wall friction, and the flow is not of axial-symmetry, and its center line is also spiral. And there is downward flow near the outside of an exit pipe, which is called the secondary flow (Fig. 2.16). The velocity near the center line does not change by the position.

d. Effects of inserted length of exit pipe *l*

The flow is not much influenced by the inserted length of an exit pipe, but the downward secondary flow takes place always near its outside. And there is the maximum velocity near the lower end of exit pipe (Fig. 2.17).

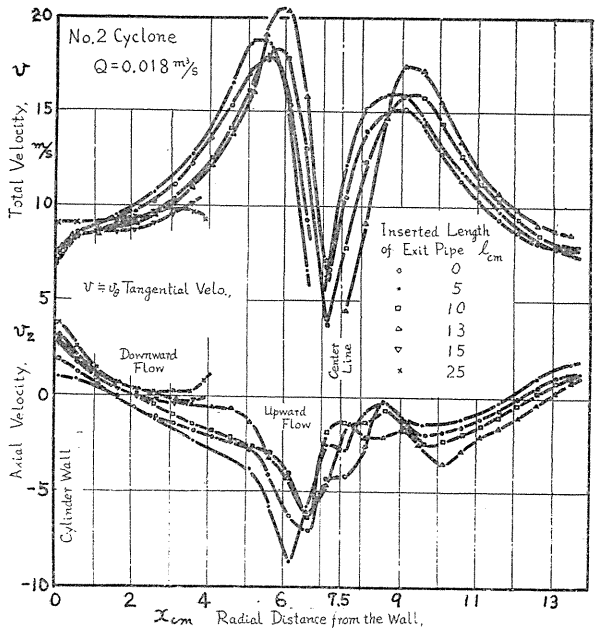

FIG. 2.17. Effects of inserted lengths of exit pipe on the velocities.

e. Effects of the forms of inlet part

Tangential and spiral inlet do not give any distinct difference in flow substantially. Most inlet guide vanes, as well as other inner obstacles,[8) 9)] reduce flow velocities, pressure drops and collection efficiencies.

f. Horizontal type

This type was developed by Linden,[14)] and the flow velocity in this type as well as those in types with other inner obstacles is reduced. And the radial distributions of tangential velocities v_θ are almost constant. The pressure drop P_i and the collection efficiency η are also lower than in the usual type, but the spiral angle θ and the axial velocity v_r become larger.

g. Effects of opening and closing of dust port

The effects are comparatively small in the pressure type cyclone, but the axial upward flow near the center is augmented by suction flow from the dust port, when it is opened (Fig. 2.18).

Opening of the dust port of the suction type must be avoided absolutely.

h. Effects of inlet and exit areas

Peripheral velocity depends upon the inlet area, and the position of the maximum velocity depends upon exit radius. The larger the inlet area becomes, or the smaller the exit area becomes, the larger the pressure drop grows (Fig. 2.19).

i. Suction type

Flow patterns in this type are substanntially the same as those of the pressure (delivery) type, though the absolute pressure is lower (Fig. 2.9).

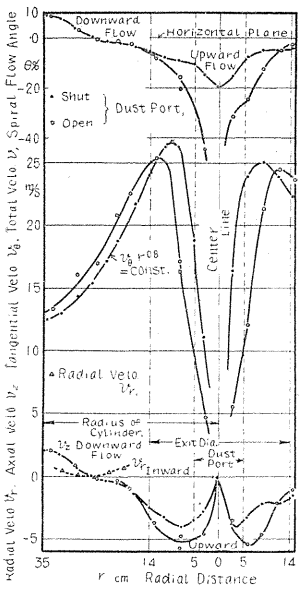

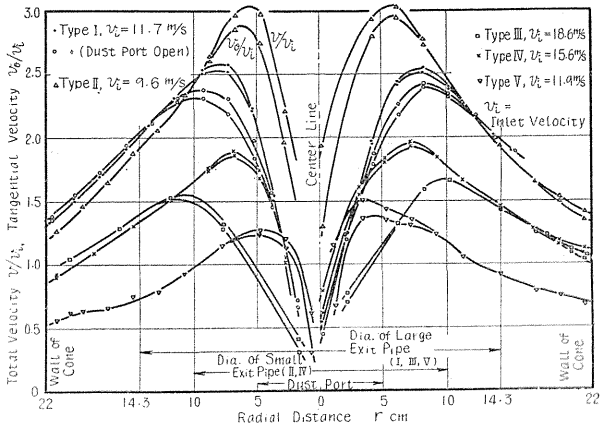

FIG. 2.18 (*left*). Distributions of spiral angles $\theta°$ and flow velocities, v, v_θ, v_z, v_r (No. 7 Cyclone).

FIG. 2.19 (*right*). Velocity distributions (v/v_i, v_θ/v_i) of various types at the conical part (No. 8 Cyclone).

4. Note on the Measured Results of Radial Velocity

The radial velocity components v_r of air flow in a cyclone were measured with spherical Pitot tubes having five holes. The small eccentricity between the center of rotating flow and the center line of the axis of a Pitot tube gave a large apparent error on the radial velocity component v_r. The values of the eccentricity and the flow tendency were obtained from measured results. The eccentricity "***a***" was an error frequently happened about the Pitot tube setting.

If the eccentricity is equal to a for the purely rotational flow ($v_r=0$), the measured results are as follows:

A. Forced Vortex. ($\omega=$const.)

In Fig. 2.20, the velocity of the point P is $v_1''=\sqrt{a^2+r^2}\cdot\omega$, and $\tan\beta_1'=a/r$, where β_1' is an apparent measured radial flow angle. The apparent measured rotational velocity v_{θ_1} and radial velocity v_{r_1} are as follows:

$$v_{\theta_1} = v_1'' \cos\beta_1' = \sqrt{a^2+r^2}\cdot\omega \times \frac{r}{\sqrt{a^2+r^2}} = r\cdot\omega, \qquad \text{(forced vortex)}$$

$$v_{r_1} = v_1'' \sin\beta_1' = \sqrt{a^2+r^2}\cdot\omega \times \frac{a}{\sqrt{a^2+r^2}} = a\cdot\omega = \text{const.}$$

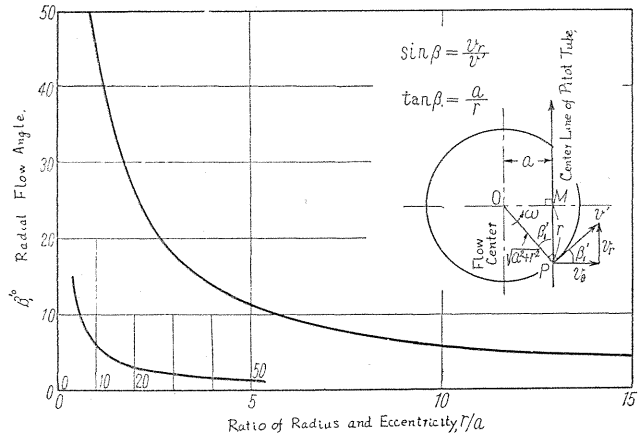

FIG. 2.20. Apparent radial flow angles by the eccentricity of the flow center.

B. *Free Vortex*

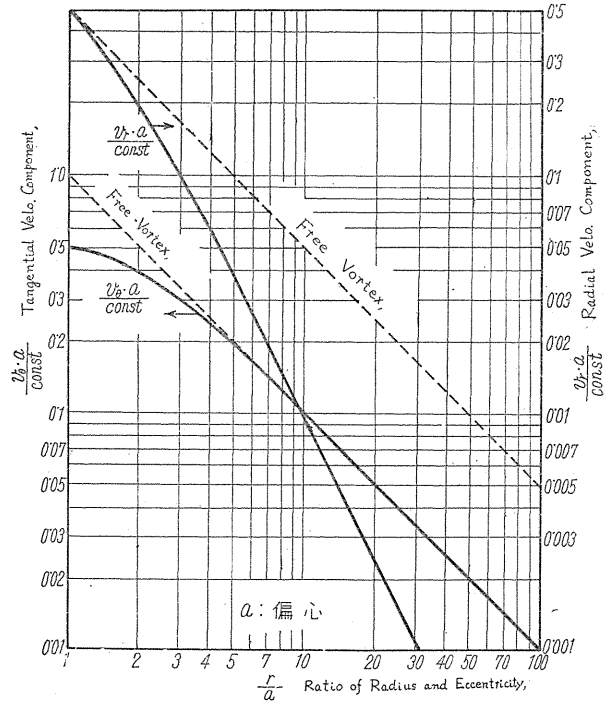

FIG. 2.21. Apparent velocity distributions by the eccentricity of the flow center.

$$v_2'' = c/\sqrt{a^2+\ ^2}, \qquad (c = \text{const.})$$

$$v_{\theta_2} = v_2'' \cos\beta_1' = \frac{c}{\sqrt{a^2+r^2}} \cdot \frac{r}{\sqrt{a^2+r^2}} = \frac{cr}{a^2+r^2} = \frac{c}{a} \frac{r/a}{(1+(r^2/a^2))},$$

$$v_{r_2} = v_2'' \sin\beta_1' = \frac{c}{\sqrt{a^2+r^2}} \cdot \frac{a}{\sqrt{a^2+r^2}} = \frac{ca}{a^2+r^2} = \frac{c}{a} \frac{1}{(1+(r^2/a^2))},$$

These results are shown in Fig. 2.21, and the apparent radial velocity component v_{ri} and the apparent radial flow angle β_1' have reverse signs to each other on the opposite sides of the center along the diameter. The angle β_1' has a larger value near the center, and therefore the eccentricity a is obtained from the measured results. It must be noticed that the angle β_1' and the velocity component v_{ri} have readily very large apparent values, because the ratio r/a can easily reach even about five (Fig. 2.22). An example of the forced vortex is the flow in the exit pipe, where the measured apparent radial velocities v_{r1} are constant as in the above formula (Fig. 1.9 and 2.13).

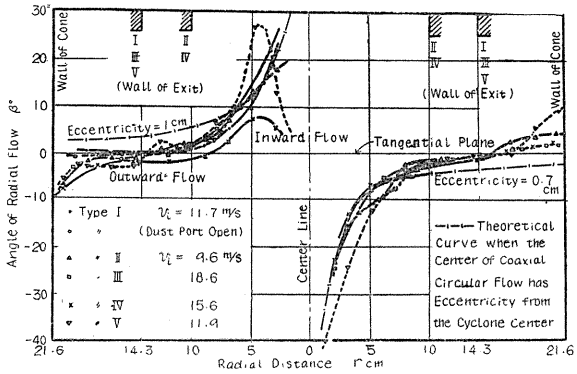

FIG. 2.22. Distributions of radial flow angles β in various types at the conical part (No. 8 Cyclone).

5. CONCLUTIONS

Air flows in many types of cyclone dust collectors were measured with cylindrical and spherical Pitot tubes. As a result of the experiments, when air flows into a cyclone, the air velocity at the inlet is accelerated or decelerated according to the inlet area, and is reduced by the wall friction of the cylindrical part, flowing spirally downwards to the bottom of the cylindrical part. Then the stream becomes centripetal at the conical part, and is accelerated nearly to such as the free vortex, and goes spirally upwards into the central exit pipe. The spiral angle θ at the periphery is about 10°, and its radial distributions show themselves to derease linearly to the center. The effects on the air flows of lengths and diameters of the cylindrical part and the exit pipe inserted, as well as the angle of cone, flow quantities, inlet area and many other forms of the cyclone (dust port, inlet part, horizontal type, suction type) were examined.

The errors of the Pitot tubes were tested and discussed, and the radial velocity components had small values in reality, but its apparent value according to the flow eccentricity was comparatively large.

Chapter III. Pressure Drop of Cyclone

1. Preliminaries

Pressure drop ΔP of the cyclone is its important item together with its collection efficiency, because the blower, which is used for the cyclone, must be selected according to the pressure drop, and the necessary energy (power input) depends upon the pressure drop and the air quantity. Theoretical formulae were derived after many observations of flow patterns in cyclones and experiments on the pressure drops had been made, and an approximately simplified formula having no dimensions was also presented. They were examined and discussed in view of many experimental results.

The pressured drop is now defined as the inlet static pressure P_i, when the exit pipe opens to the atmospheric pressure. The difference $(P_i\text{-}P_e)$ between the inlet static pressure and the static pressure on the exit pipe wall is smaller by 20-30% than the inlet static pressure or the true pressure loss, because the static pressure P_e on the wall of the exit pipe is higher than the mean pressure of the outlet owing to the centrifugal force of the rotating flow in the exit pipe.

The pressure drop of a cyclone is proportional to the square of air quantity, and the pressure of a blower decreases gradually as the air quantity increases at the same speed of the blower. An operating point is a crossing point of the two pressure characteristics.

Therefore, if the speed of the blower changes by chance, the pressure change is larger than the change of flow quantity, and on the contrary, if the pressure drop of a cyclone is changed, the pressure change is smaller than the change of flow quantity on the whole.

2. Experimental Results

A. Effect of Length of Cylindrical and Conical Parts. (L and H)

A longer cylinder or cone has larger friction loss than a shorter one, and the friction reduces air velocity and centrifugal force. Therefore the cyclone of a longer cylinder or cone gives lower pressure loss, which is inversely proportional to the square root of its total length (Fig. 3.1).

A cylindrical part elongated upwards above the inlet pipe of a cyclone has a little effect on its pressure drop, and the loss is almost inversely proportional to the fourth root of the total length of the cylindrical and conical parts.

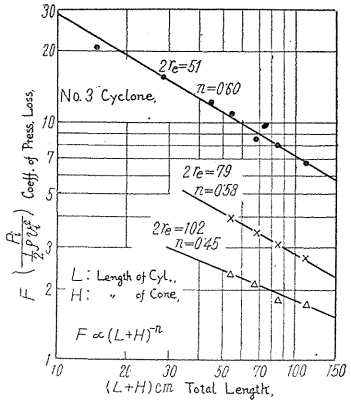

FIG. 3.1. Effect of cyclone length.

B. Effect of Radius of Exit Pipe. (r_e)

This effect on the pressure drop is inversely proportional to the square of the radius r_e regardless of the cone angles. And Mr. Shepherd showed the same results[8] (Fig. 3.2).

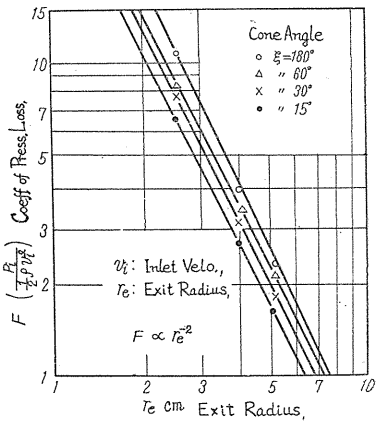

FIG. 3.2. Effect of exit radius.

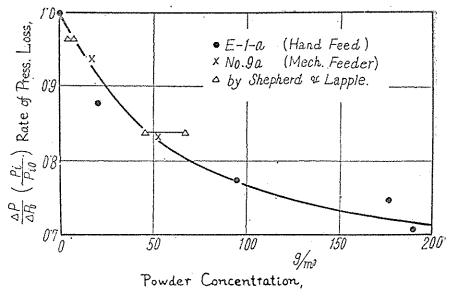

FIG. 3.3. Effect of powder concentration.

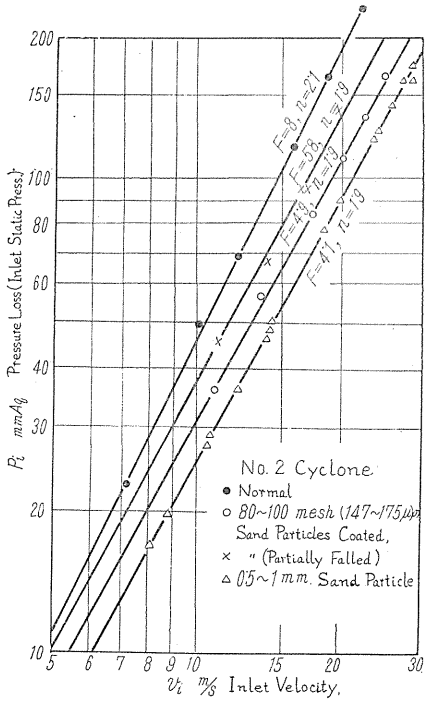

FIG. 3.4 (*left*). Effect of wall friction.

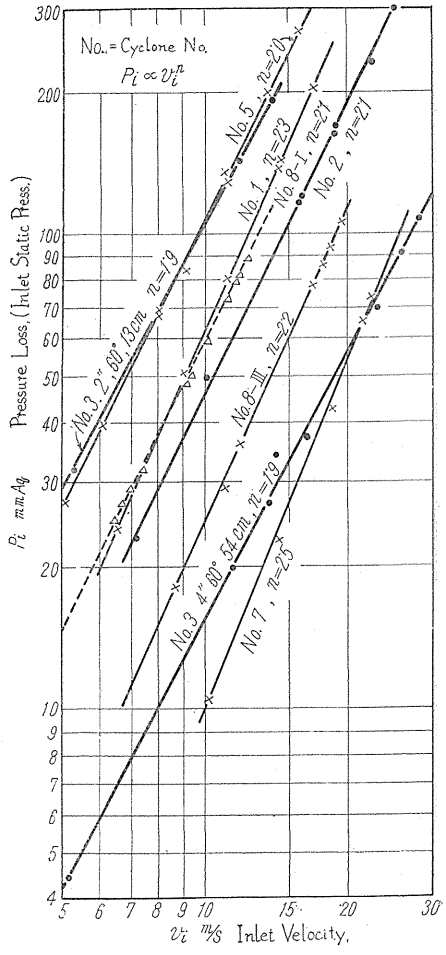

FIG. 3.5 (*right*). Effect of inlet velocity.

C. Effect of Concentration of Test Powder

When air flow is charged with some quantity of a test powder, the pressure drop of the cyclone becomes smaller than that for pure air flow (no test powder) (Fig. 3.3). This decrease will be almost unaffected by types and dimensions of cylclones. I think that its reason is the increase of friction coefficient in the cyclone due to powder particles.

D. Effect of Wall Friction in a Cyclone

The friction was changed by pasting sand particles of definite sizes on the wall. The pressure loss of a cyclone is greatly influenced by the friction loss, and the larger wall friction is the smaller pressure drop becomes (Fig. 3.4), but this is a phenomenon reversed to what common sense understands.

E. Effect of Air Velocity or Air Quantity

Pressure loss is generally proportional to the square of inlet velocity, but strictly speaking, the exponent of the inlet velocity changes from about 1.8 to 2.3. Therefore the coefficient F of the pressure loss is not constant with the inlet air velocity or air quantity (Fig. 3.5).

F. Calculation of the Pressure Drop by Measured Velocity Distribution in a Cyclone

As the losses of inlet part and exit pipe are small, the actual pressure loss is found to be almost equal to a integrated value of air centrifugal force ($\rho v_\theta^2/r$) from the radius ($0.6\ r_e$) of zero static pressure to the radius (R) of the cylindrical part in many experiments.

$$\Delta P \fallingdotseq P_i \fallingdotseq \rho \int_{0.6r_e}^{R} (v_\theta^2/r)dr \fallingdotseq 0.12 \sum_{0.6r_e}^{R} (v_\theta^2/r)dr,$$

G. Effect of Inner Obstacles

When there are any inner obstacles (bar, plate, disc, vane and Pitot tube) in a cyclone, its pressure loss becomes lower, because the tangential velocity v_θ is reduced by the drag of the obstacle. The magnitude of the decrease is roughly proportional to the product of air velocity and the projected frontal area of the obstacle.

H. Effect of Inserted Length of Exit Pipe

This effect is small and negligible in general.

I. The Difference ($P_i - P_e$) between Inlet Static Pressure (P_i) and Static Pressure (P_e) on Exit Wall

This difference is lower by 20-40% than P_i, and may not be affected by shutting and opening of the dust port. But it is difficult to estimate this value exactly.

3. An Approximate Formula

A. A New Formula

A new approximate formula for the pressure loss of a cyclone is obtained from the above experiments, but this formula does not contain a variable coefficient of the wall friction.

$$F_3=\frac{P_i}{\frac{1}{2}\rho v_i^2}=\frac{30\,a\sqrt{D}}{d^2\sqrt{L+H}}.$$

The maximum difference between this calculated value (F_3) and the experimental result (F_m) is comaratively small and about 30-40% in normal types (Table 3.1).

TABLE 3.1. Measured and Calculated Values of Pressure Losses in Various Cyclones (at the inlet velo. $v_i=10$ m/s).

Cyclone No.	D (cmϕ)	a (cm^2)	d (cmϕ)	$L+H$ (cm)	F_m	F	F_3	F_4	Remarks
1	30	16.5	5	77	11	8	13	14	
2	15	15	5	37	8	10	12	14	
3 $\frac{\text{E}}{15^\circ}\frac{\text{d}}{2''}$	18.2	○20.6	5.1	111	7	8	10	9	○Circular inlet
3 15° 3″	〃	〃	7.9	〃	2.7	3.4	4.0	3.8	
3 15° 4″	〃	〃	10.2	〃	1.7	2.1	2.4	2.2	
3 $\frac{\text{L}}{30^\circ\ 2''\ 15\text{ cm}}$	〃	〃	5.1	44	13	15	16	17	
3 30° 2″	〃	〃	〃	83	8	8	11	11	
3 30° 3″	〃	〃	7.9	〃	3.1	4.0	4.6	4.7	
3 30° 4″	〃	〃	10.2	〃	1.8	2.4	2.8	2.8	
3 60° 2″ 15 cm	〃	〃	5.1	28	16	17	20	23	
3 60° 2″	〃	〃	〃	67	9	10	12	15	
3 60° 3″	〃	〃	7.9	〃	3.4	4.3	5.1	6.1	
3 60° 4″	〃	〃	10.2	〃	2.1	2.5	3.2	3.7	
3 180° 2″ 15 cm	〃	〃	5.1	15	21	18	26	—	
3 180° 2″	〃	〃	〃	54	11	10	14	—	
3 180° 3″	〃	〃	7.9	〃	4.0	4.3	6	—	
3 180° 4″	〃	〃	10.2	〃	2.3	2.5	3.4	—	
4 a	28.4	×100	11.6	70	19	18	14	16	×Spiral inlet
4 b	〃	〃	6.4	〃	57	56	46	53	
4 a′	〃	〃	11.6	60	8	—	—	—	Horizontal
5	14.5	×30	5.9	38	18	20	16	18	
6	125	×2.500	55	335	19	19	15	17	
7	70	×180	28	150	(3)	5	5	6	( ) Inaccurate
8-I	55	440	28.5	240	10	11	8	9	
8-II	〃	〃	20	〃	20	22	16	17	
8-III	〃	220	28.5	〃	4.0	5	3.5	4.3	
8-VI	〃	〃	20	〃	8	10	8	9	
9 a	6.5	×6.3	3	20	11	12	12	13	
9 b	〃	6.3	3	〃	7	10	13	—	Without cone
10	14	45	7	40	14	15	17	17	

Key: F_m=Measured value, F=Theoretically calculated value, F_3=Approximately calculated value, F_4=First's formula.

B. Discussion on Approximate Formulae already proposed

a) First's formula [10)23)]

$$F_4=\frac{12\,a}{cd^2}\Big/\left(\frac{LH}{D^2}\right)^{1/3},$$

where c: Factor, =0.5 (without inlet vane)
=1.0~2.0 (with inlet guide vane)

This formula is the best of many formulae already proposed, and gives a value near to what the above new formula gives. But when L or H is zero, F_4 becomes unreasonably infinite.

b) Other formulae

Formulae proposed by others contain many assumptions and irrational factors, and give erroneous values.

4. A Theoretical Formula of Pressure Drop

In a cyclone the inlet velocity (v_i) is accelerated or deccelerated to the velocity (v_1) at the radius (r_1) of the cylinder top according to the ratio of inlet area (a) and the cross sectional area of cylinder (πR^2), and is decreased to the velocity (v_2) at the radius (r_2) of the cylinder bottom due to cylinder wall friction, and v_2 is increased to the velocity (v_3) at 60% radius (0.6 r_e) of the exit pipe by centripetal flow (Fig. 3. 6). As static pressure in the cyclone of delivery type is zero at the same radius (0.6 r_e), and as static pressures on the cylinder wall are almost equal at any point, and as pressure loss of upward flow in the center zone of the cyclone is negligible, the following formulae are obtained.

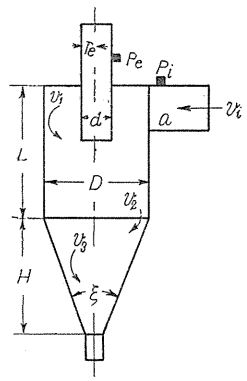

FIG. 3. 6. Symbols of air flow in a cyclone.

A. The velocity (v_1) is given from the following formulae by many experimental results

$$\left.\begin{aligned} &\sqrt{a}/2R<0.35, && \cdots\cdots\ v_1/v_i=1.40,\\ &0.35>\sqrt{a}/2R>0.20, && \cdots\cdots\ v_1/v_i=4\sqrt{a}/2R,\\ &0.20>\sqrt{a}/2R, && \cdots\cdots\ v_1/v_i=0.80, \end{aligned}\right\} \qquad (1)$$

B. Decceleration on the Wall of the Cylindrical Part

Air flow quantity, $G=\rho Q=av_i\rho$,

From balance of rotational momenta, taking account of the wall friction,

$$v_1Gr_1=v_2Gr_2+f_1\rho RA\frac{v_1^2+v_2^2}{2},$$

and put

$$k=\frac{f_1ARv_1}{2ar_1v_i},$$

where r_1: Radius of air flow having the velocity (v_1) at the top of the cylindrical part (cm),

r_2: Radius of air flow having the velocity (v_2) at the bottom of the cylindrical part (cm),

f_1: Friction coefficient of the cylinder wall,

A: Total area of inner surface of the cylindrical part (cm^2) $=\pi DL$,

then

$$k\left(\frac{v_2}{v_1}\right)^2+\frac{r_2}{r_1}\left(\frac{v_2}{v_1}\right)+k-1=0,$$

$$\therefore\quad \frac{v_2}{v_1}=\frac{-(r_2/r_1)+\sqrt{(r_2/r_1)^2-4k(k-1)}}{2k}, \qquad (2)$$

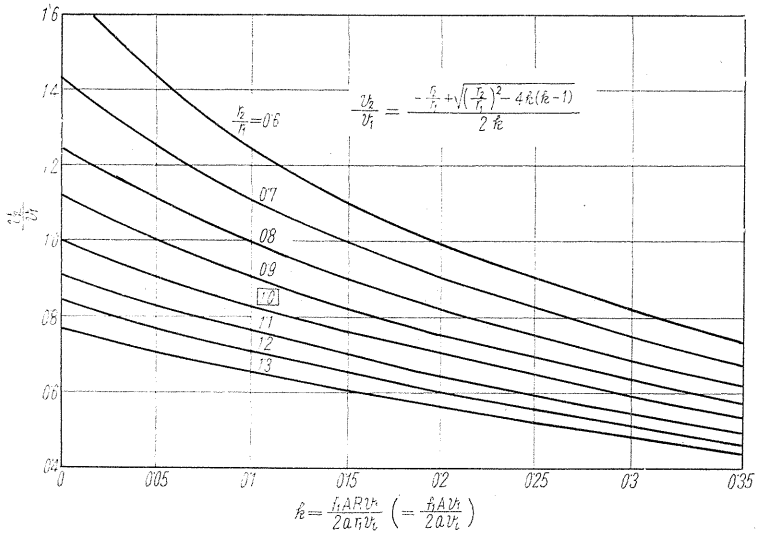

FIG. 3.7. Calculation diagram of deceleration on the cylinder wall.

This value is shown in Fig. 3.7, and generally $r_2/r_1=1.0$,

$$\therefore \quad v_2/v_1=\frac{-1+\sqrt{1-4k(k-1)}}{2k}, \tag{2'}$$

and k is calculated from the following equations, which are derived from the equations (1),

$$\left.\begin{aligned} &\sqrt{a}/D>0.35, && \cdots\cdots k=0.7\pi f_1DL/a,\\ &0.35>\sqrt{a}/D>0.20, && \cdots\cdots k=2\pi f_1L/\sqrt{a},\\ &0.20>\sqrt{a}/D, && \cdots\cdots k=0.4\pi f_1DL/a, \end{aligned}\right\} \tag{3}$$

The difference between a spiral inlet and a tangential inlet is negligible, and the friction coefficient f_1 is assumed to be twice as large as that of a flat plate in a parallel turbulent flow (Fig. 3.8).

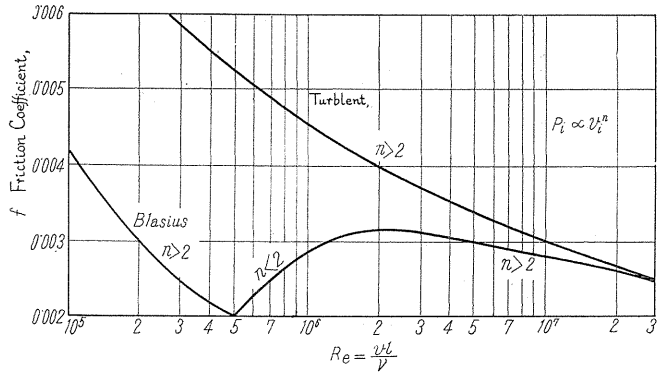

FIG. 3.8. Friction coefficient of cyclone wall.

This method is similar to Mr. Stairmand's one, and his friction coefficient is 1/200.[17]

C. Acceleration of the Centripetal Flow at the Conical Part

The increase of air velocity is given in the equation $vr^n=c$, $(n<1)$. From balance of rotational momenta, the following equations are obtained (Fig. 3.9).

$$Gv_2r_2 = Gv_3r_3 + \frac{2\pi f_2\rho}{\sin(\xi/2)}\int_{r_3}^{R} v^2r^2dr,$$

where f_2 is a coefficient of wall friction at the conical part.

$$\therefore\ v_2r_2 = v_3r_3 + \frac{2\pi f_2\rho c^2}{G(3-2n)\sin(\xi/2)}(R^{3-2n} - r_3^{3-2n}),$$

Substituting $G=a\rho v_i$, and $v_2r_2^n = v_3r_3^n$ in the above formula,

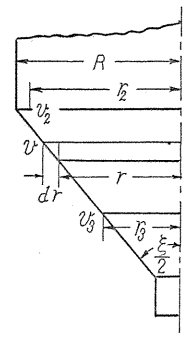

FIG. 3.9. Symbols of the conical part.

$$\frac{\sin(\xi/2)}{2f_2}\cdot\frac{v_i}{v_2}\cdot\frac{a}{\pi r_3^2} = \frac{(r_2/r_3)^n\{(R/r_3)^{3-2n}-1\}}{(3-2n)\{(r_2/r_3)^{1-n}-1\}},$$

Moreover, considering roughly the friction loss of the above deck of the cyclone,

$$\frac{a}{2f_2(v_2/v_i)\left(1+\dfrac{1}{\sin(\xi/2)}\right)\pi r_3^2} = \frac{(r_2/r_3)^n\{(R/r_3)^{3-2n}-1\}}{(3-2n)\{(r_2/r_3)^{1-n}-1\}} = y, \qquad (4)$$

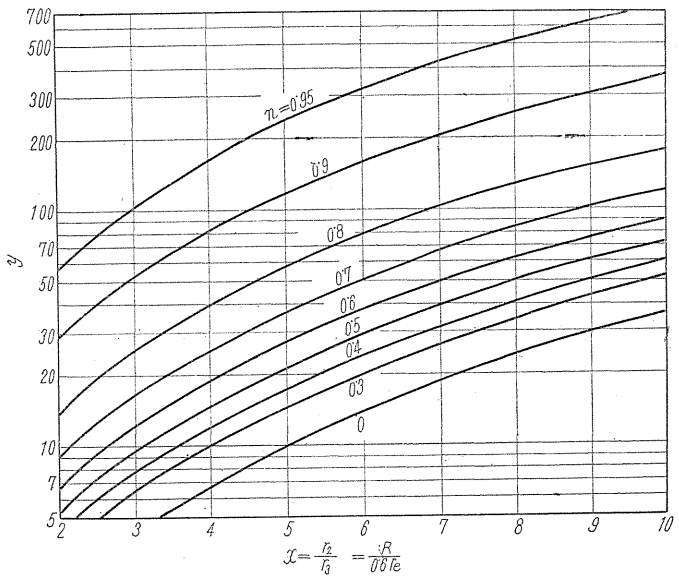

FIG. 3.10. Calculation diagram of air flow in the conical part.

The left hand term of the above equation can be calculated, and the exponent n can be obtained. As static pressure in the cyclone is zero at 60% radius of the exit pipe, generally $r_2=R$, $r_3=0.6\,r_e$, and $x=r_2/r_3=R/0.6\,r_e$.

The graphical solution of this equation in Fig. 3.10 is convenient. The friction coefficient f_2 of the conical wall may be assumed to be equal to f_1, and Reynolds number R_e may be put to be $6\,(L+H)v_i/\nu$ (Fig. 3.8).

D. Pressure Loss

Pressure loss is given to be the static pressure in the inlet pipe of the cyclone of pressure type.

$$\Delta P = P_i = \int_{0.6\,r_e}^{R} \rho(v_0^2/r)dr,$$

The tangential velocity v_0 is approximately equal to the total velocity v, and static pressures on the cylinder wall are almost the same at any point, and $v_2 r_2^n = v r^n$, then the following formula is obtained.

$$P_i = \frac{\rho v_2^2}{2n}\{R/0.6\,r_e)^{2n}-1\} = \frac{\rho}{2n}(v_3^{2n}-v_2^{2n}), \tag{5}$$

Thus the pressure loss can be calculated theoretically.
The coefficient of pressure loss is given as follows:

$$F = p_i \Big/ \left(\frac{1}{2}\rho v_i^2\right).$$

5. A Numerical Example

A. A Numerical Example of the Pressure Loss for No. 4 Cyclone (Linden type)

$(L+H)=70$ cm, $L=23$ cm, $a=100$ cm^2, $D=28.4$ cm,
$r_e=5.8$ cm, $\xi=25°$, $\nu=0.15$ cm^2/s,

The pressure loss is calculated at the inlet velocity $v_i=10$ m/s.

$$R_e=6(L+H)v_i/\nu=6\times70\times1{,}000/0.15=2.8\times10^6,$$

From Fig. 3.8, $f=0.0038$,
and

$$\sqrt{a}/D=\sqrt{100}/28.4=0.352, \qquad \therefore \text{ by (1)}, \quad v_1/v_i=1.40,$$
$$k=0.0038\,\pi\times28.4\times23\times1.40/200=0.055,$$

$\therefore$ from Fig. 3.7, or (1′), $v_2/v_1=0.90$,

$$R/0.6\,r_e=14.2/0.6\times5.8=4.1,$$
$$\therefore\ y=100/(2\times0.0038\times0.90\times1.40\times5.62\times0.36\,\pi\times33.5)=49,$$

$\therefore$ from Fig. 3.10, or (4), $n=0.82$,

$$\therefore\ F=P_i/\tfrac{1}{2}\rho v_i^2=(1.40\times0.90)^2(4.1^{2\times0.82}-1)/0.82=18,$$

and on the other hand, $F_3=30\times100\sqrt{28.4}/(11.6^2\times\sqrt{70})=14$.
The measured value $F_m=19$ is almost consistent with the calculated value $F=18$, and nearly with the approximate value $F_3=14$.

B. Effect of Reynolds Number (Air Velocity)

As flow quantity or inlet air velocity varies, Reynolds Number and consequently friction coefficient change themselves, and therefore pressure loss is not exactly proportional to the square of air velocity, and the coefficient F of pressure loss is not constant.

A numerical example for No. 2 cyclone gives $P_i \propto v_i^{2.13}$, and the particulars of it are as follows:

$v_i =$	5	10	15	(m/s),
$f =$	0.0048	0.0043	0.0037	
$F =$	9.2	10.3	11.4	
$P_i =$	14	62	273	(mm Aq).

C. Effect of Friction Coefficient

As the friction coefficient in a cyclone grows twice, the pressure loss becomes about a half. A practical example is shown in Fig. 3.4, and a numerical example for the same cyclone is given in Fig. 3.11.

D. Comparisons with Measured Values

Comparisons between the values of pressure losses theoretically calculated and those experimentally measured are given on many test cyclones in Table 3.1, and show good agreements among them in spite of the approximate assumptions.

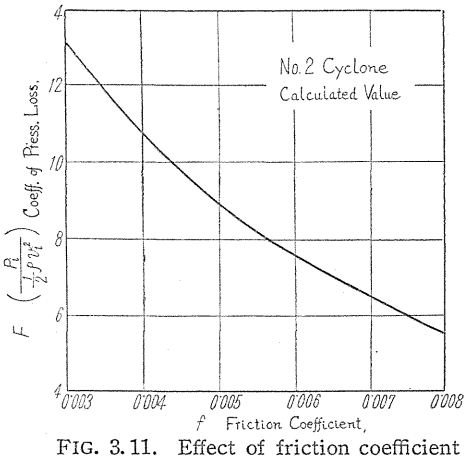

FIG. 3.11. Effect of friction coefficient on pressure loss of No. 2 cyclone.

6. CONCLUSION

Results of many systematic experiments and a method of theoretical calculation on pressure loss of the cyclone were obtained, and good agreements between experiments and the theory were shown.

This theory may make it easy to design a new cyclone and to estimate its characteristics. An approximate simple formula for pressure loss was also obtained.

Symbols

P_i : Static pressure in the inlet pipe (mm Aq),
ρ : Air density ($\fallingdotseq 0.12$ under the standard condition) (kg.s^2/m^4),
v_i : Air velocity in the inlet pipe (m/s),
a : Inlet area (cm^2),
D : Diameter of cylindrical part (cm) $= 2R =$ Cyclone dia.,
d : Diameter of exit pipe (cm) $= 2r_e$,
L : Length of cylindrical part (cm),
H : Length of conical part (cm),
b : Width of inlet port (cm),

h : Height of inlet port (cm),
v : Total velocity of air flow (m/s),
v_θ : Tangential velocity of air flow (m/s),
v_z : Axial velocity of air flow (m/s),
v_r : Radial velocity of air flow (m/s),
r : Radius (cm),
P_e : Static pressure on the wall of exit pipe (mm Aq.),
F : Coefficient of pressure loss,
F_m: Measured coefficient of pressure loss,
G : Weight quantity of air flow,
Q : Volume quantity of air flow,
f : Friction coefficient of the wall,
ξ : Cone angle,
n : Exponent for the vortex,
ν : Kinematic viscosity of air (cm^2/s),

Chapter IV. Collection Efficiency of Cyclone

1. Preliminaries

Collection efficiency is the most important character of the cyclone dust collector. The dust particles are sedimentated on to the cyclone wall by centrifugal force (v_0^2/r), and are collected at the bottom by air flow and gravity, and are taken out from the dust chamber. As the diameter of the particles in question is about 1~10 μ, Stokes' law or Allen's law is applicable to the particle motion in this case. Air flow pattern in the cyclone has already been made clear in the previous chapters.

On the other hand, the size distributions of test powder are also important, and are measured by two sedimentation methods (Andreasen and Kelly), and by an air elutriation method. Blaine's air permeability method gives the specific surface area of the powder. The shapes of the particles are observed by the microscopic photographs.

But the particles are often coagulated and the interference sedimentation may happen in the cyclone, therefore the absolute value of the collection efficiency cannot be calculated theoretically, but the relative comparison of the efficiency can be done by this theory.

And also the author have experimented on collection efficiencies of various types of cyclones, and discussed these results in view of my theory.

2. Experimental Apparatus and Measuring Methods

1. Experimental Apparatus

A. Collection Efficiency

The apparatus are the same as those for flow measuring except the feeder of test powder. The feeder for delivery type has a Venturi tube, in which the flow pressure is slightly negative, but the suction type does not need any special device. (Fig. 4.1)

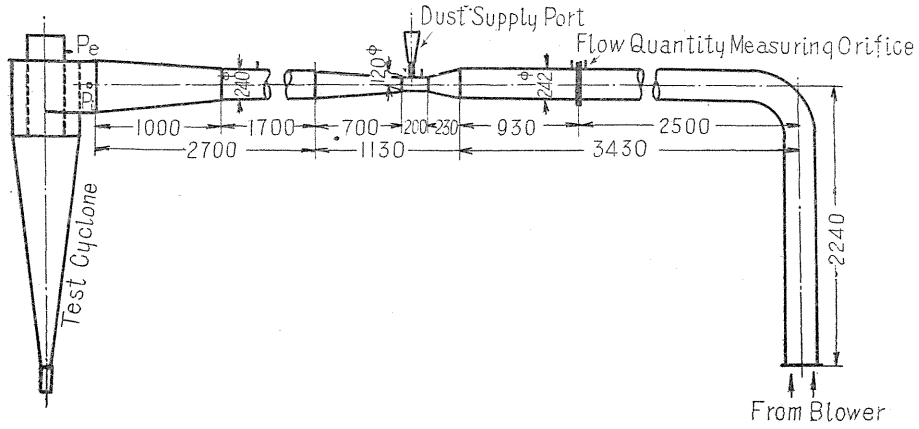

FIG. 4.1. An experimental apparatus.

B. Size Distribution of Test Powder

The measuring methods for size distribution used are as follows:

a) Andreasen's pipette,
b) Kelly's tube (Wigner's method),
c) Air elutriation method,
d) Microscopic photograph,
e) Blaine's specific surface meter,

a and b are used in the field of ceramic industry, and c is the reconstruction of that for cement industry.

1. Test Powder

Test Powder should be fine particles which give a low efficiency even for a small cyclone, because the difference among collection efficiencies is too small to compare themselves, when all efficiencies are high. And it is convenient to be little adhesive and uncoagulated, and not to be affected by atmospheric humidity, and to be able to be obtained in large quantities.

Various carborundums, cement, cement raw material, diatomaceous earth, pulverized coal, various clays, kaolin, wheat-flour, soda-ash, Grauber's salt, various calcium carbonates, various flue dusts, tooth powder, carbon black, basic magnesium carbonate etc. were examined, but talc was found to be the most convenient and dolomite was also used. The size distribution of talc powder is shown in Fig. 4.2.

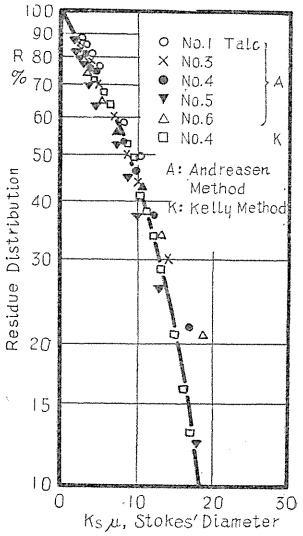

FIG. 4.2. Size distribution of talc powder.

2. Measuring Method

The measuring methods for air flow quantity and pressure were the same as in the previous chapter.

When the inlet velocity is low (about 7 m/s), the powder stays in the inlet pipe and on the cyclone wall. Therefore, after the powder in the dust chamber is taken out, the highest inlet velocity is applied to blow down the clinged powder. Then the modified collection efficiency (η_c) of the cyclone becomes as follows:

$$\eta_c = \frac{W}{W_0 - w/\eta_m}$$

where W_0: Supplied quantity of powder (30~400 g),
W : Collected quantity of powder at the first inlet velocity,
w : Collected quantity of powder at the succeeding highest velocity,
η_m: Collection efficiency of the cyclone at the highest inlet velocity.

3. A Theory of Collection Efficiency and Its Discussion

1. Sedimentation Velocity

The terminal velocity of a spherical particle under the gravity is obtained by the Stokes' formula, and the velocity under a centrifugal force v_θ^2/r becomes as follows:

$$v_{rs} = \frac{\delta^2(\rho_s - \rho_0)v_\theta^2}{18\ \mu r} \times 10^{-8} \fallingdotseq \frac{\delta^2 \rho_s v_\theta^2}{18\ \mu r} \times 10^{-8},$$

where v_{rs}: Terminal settling velocity at the radius r (cm/s),
δ : Diameter of the particle (Stokes' dia.) ($\mu = \mathrm{cm}^{-4}$),
ρ_s : Density of the particle (g/cc),
ρ_0 : Density of gas (Surrounding medium) (g/cc),
μ : Static viscosity of gas (g/cm.s),
v_θ : Tangential velocity of the particle at the radius r (cm/s),
r : Rotating radius of the particle (cm).

The tangential velocity of the particle is assumed to be equal to that of air flow.

If the Reynolds number is large, it is adequate to apply the Allen's formula, then the above formula becomes as follows:

$$v'_{rs} = \left\{ \frac{4}{225} \frac{\rho_s^2}{\rho_0} \frac{v_\theta^4}{\mu r^2} \right\}^{1/3} \delta \times 10^{-4},$$

The limiting size of powder in a cyclone between Stokes' and Allen's law is about $\delta = 5\ \mu$.

2. The Critical Diameter of the Dust Particle for the Separation. (Cut Size)

When the radial velocity v_r of air flow in a cyclone is equal to the settling velocity v_{rs}, the particle is neither collected nor exhausted. Therefore its diameter δ is the balanced diameter δ_0 at the point in the cyclone.

On the other hand, from the experimental results

$$v_0 r^n = k_1 = \text{const.}, \qquad (n < 1)$$

$$\therefore \quad \delta^2 = \frac{18\,\mu}{\rho_s k_1^2}(v_r r^{2n+1}) \times 10^8, \qquad \text{(Stokes)}$$

or

$$\delta = \left\{ \frac{225}{4} \frac{\rho_0}{\rho_s^2} \frac{\mu}{k_1^4} \right\}^{4/3} v_r r^{\frac{2+4n}{3}} \times 10^4, \qquad \text{(Allen)}$$

Moreover,

$$v_r r^m = k_2 = \text{const.}, \qquad (m = 0 \sim 1)$$

$$\therefore \quad m = 0; \quad v_r = k_2,$$

$$\delta^2 = \frac{18\,\mu k_2}{\rho_s k_1^2} r^{2n+1} \times 10^8, \qquad \text{(Stokes)}$$

or

$$\delta = \left\{ \frac{225}{4} \frac{\rho_0}{\rho_s^2} \frac{\mu}{k_1^4} \right\}^{4/3} k_2 r^{\frac{2+4n}{3}} \times 10^4, \qquad \text{(Allen)}$$

$$m = 1; \quad v_r r = k_2,$$

$$\delta^2 = \frac{18\,\mu k_2}{\rho_s k_1^2} r^{2n} \times 10^8, \qquad \text{(Stokes)}$$

or

$$\delta = \left\{ \frac{225}{4} \frac{\rho_0}{\rho_s^2} \frac{\mu}{k_1^4} \right\}^{4/3} k_2 r^{\frac{4n-1}{3}} \times 10^4, \qquad \text{(Allen)}$$

And $n = 0.5 \sim 0.8$ generally, therefore, the larger the radius r becomes, the larger the diameter δ grows. Accordingly the balanced diameter δ shows the maximum value on the cylinder wall. But if the critical diameter would exist, the repeated supply of the collected dust should show 100% collection efficiency. The experimental results do not give such repeated efficiency (100%) for the powder, which is hard to be recrushed or dispersed in a cyclone (Fig 4.3). And from many microscopic observations the critical size is proved not to exist in practice strictly. But the assumed critical size is used for the theoretical calculation of collection efficiency for the sake of convenience.

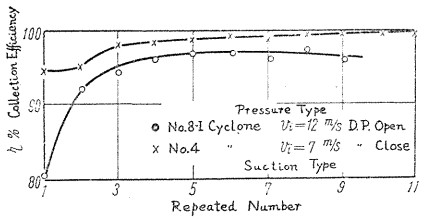

FIG. 4.3. Repeated collection efficiencies.

3. Size Distribution of Powder

The residue distributions of many kinds of powder can be generally given by the Rosin-Rammler's formula.

$$R = e^{-b\delta^n} = 10^{-b'\delta^n} \qquad (n \fallingdotseq 0.2 \sim 2.5)$$

4. Collection Efficiency

The collection efficiency is given by the following formula;

$$\eta = \int_0^\infty \Delta\eta \cdot f(\delta)\, d\delta$$

where $\Delta\eta$: Partial collection efficiency at δ, (<1)

$f(\delta) = -\dfrac{dR}{d\delta} > 0$: Distribution function of weight frequency of a dust powder,

Now the first approximation is $\eta_{1\cdot1} = R_\delta$. And the partial collection efficiency will be given by one of the following approximate formulae, according to experimental or assumed partial collection efficiencies of Fig. 4.4.

$$\left.\begin{aligned} &\Delta\eta_2 = 1 - e^{-p\delta}, \quad \Delta\eta_3 = 1 - e^{-q\delta^2}, \\ &\Delta\eta_4 = 1 - e^{-r\delta^3}, \quad \Delta\eta_5 = s\delta, \quad \Delta\eta_6 = t\delta^2. \end{aligned}\right\}$$

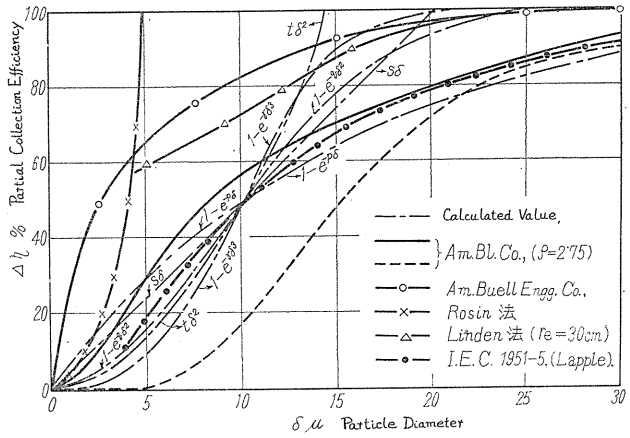

FIG. 4.4. Partial collection efficiency.

Then the total collection efficiencies for each of the above approximations are to be obtained by the following formulae respectively:

A. $R = e^{-b\delta}$

a) $\Delta\eta_2$; $\eta_{1,2} = p/(p+b)$, (2nd approximation)

b) $\Delta\eta_3$; $\eta_{1,3} = 1 - \dfrac{\sqrt{\pi}}{2}\dfrac{b}{\sqrt{q}} e^{b^2/4q}$, (3rd approximation)

c) $\Delta\eta_5$; $\eta_{1,5} = \dfrac{s}{b}(1 - e^{-b/s})$, (5th approximation)

d) $\Delta\eta_6$; $\eta_{1,6} = \dfrac{2t}{b^2} - 2e^{-b/\sqrt{t}}\left(\dfrac{\sqrt{t}}{b} + \dfrac{t}{b^2}\right)$, (6th approximation)

B. $R = e^{-b\delta^2}$

a) $\Delta\eta_2$; $\eta_{2,2} = 1 - e^{p^2/4b}\left(1 - \dfrac{p}{\sqrt{b}}\dfrac{\sqrt{\pi}}{2}\right)$,

b) $\Delta\eta_3$; $\eta_{2,3} = q/(b+q)$,

c) $\Delta\eta_6$; $\eta_{2,6} = t/\{b(1 - e^{-b/t})\}$,

C. $R = e^{-b\sqrt{\delta}}$

a) $\Delta\eta_2$; $\eta_{1/2,2} = 1 - \dfrac{\sqrt{\pi}}{2}\dfrac{b}{\sqrt{p}} e^{b^2/2p}$,

b) $\Delta\eta_5$; $\eta_{1/2,5} = 2\dfrac{s}{b^2} - 2e^{-b\sqrt{s}}\left(\dfrac{\sqrt{s}}{b} + \dfrac{s}{b^2}\right)$,

c) $\Delta\eta_6$; $\eta_{1/2,6}=\dfrac{24\,t}{b^4}-4e^{-b^{1/4}\sqrt{t}}\left(\dfrac{t^{1/4}}{b}+3\dfrac{t^{2/4}}{b^2}+6\dfrac{t^{3/4}}{b^3}+6\dfrac{t}{b^4}\right)$,

A numerical example of the effect of the partial efficiency on the total efficiency is shown in Fig. 4.5. In the figures the diameter δ of powder particle is that of the partial efficiency $\Delta\eta=50\%$, and the residue distribution of powder size is assumed to be $R=10^{-\delta/30}$. The effect of the partial efficiency is small, but the effect of the size distribution is rather large. Therefore the first approximation ($\eta=R$) is sufficient and convenient for the practical use.

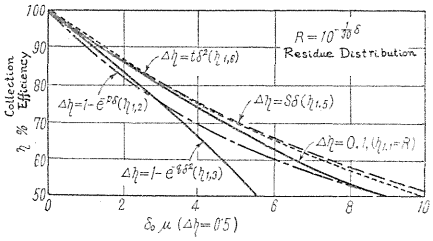

FIG. 4.5. Effect of partial collection efficiency.

5. APPLICATION OF THE THEORY

A. Effect of Inlet Velocity v_i

Since it is reasonable to assume $v_{rs}=v_r=k_3v_i$, and $v_\theta=k_4v_i$, we get from the previous formula for the critical size δ:

Stokes: $$\delta=\sqrt{\frac{18\,\mu r k_3}{\rho_s k_4^2}}\times\frac{10^4}{\sqrt{v_i}}=\text{const.}\times\frac{1}{\sqrt{v_i}},$$

Allen: $$\delta=\text{const.}\times\frac{1}{v_i^{1/3}},$$

and from the 1st approximation,

Stokes: $$\eta_{n,1}=10^{-c_1'/v_i^{n/2}},\quad\text{or}\quad\log\eta_{n,1}\propto v_i^{-n/2},$$

Allen: $$\log\eta_{n,1}\propto v_i^{-n/3},$$

When $n=1$ and Stokes' law is applied,

2nd approximation: $$\eta_{1,2}=1-\frac{1}{c_2\sqrt{v_i}+1},$$

3rd approximation: $$\eta_{1,3}=1-\frac{\sqrt{\pi}}{2}\frac{c_3}{\sqrt{v_i}}e^{c_3^2/(4v_i)},$$

5th approximation: $$\eta_{1,5}=\frac{\sqrt{v_i}}{c_5}(1-e^{-c_5/\sqrt{v_i}}),$$

And when $n=2$, the 1st approximation of Stokes' formula;

$$\eta_{2,1}=R=e^{-c_7/v_i},$$

and $n=\dfrac{1}{2}$, then $\eta_{1/2,1}=R=e^{-c_8/4(\sqrt{v_i})}$,

where c_i is a constant. A calculated example shown in Table 4.1 reveals that the effect of the partial efficiency is negligible, but that the size distribution is significant.

TABLE 4.1. Effect of the Inlet Velocity on the Collection Efficiency.

v_i (m/s)	4	7	9	10	12	16	20
$\eta_{1,1}$	84.7	88.2	89.5	90.0	90.8	92.0	92.8
$\eta_{1,2}$	85.0	88.3	89.5	〃	90.8	91.9	92.7
$\eta_{1,3}$	84.2	88.1	89.6	〃	91.0	92.2	92.9
$\eta_{1,5}$	85.2	88.2	89.5	〃	90.8	92.0	93.0
$\eta_{2,1}$	76.8	86.0	88.8	〃	91.5	93.6	94.9
$\eta_{1/2,1}$	87.6	89.2	89.7	〃	90.4	91.2	91.7
$\eta_{2/3,1}$	86.8	88.8	89.7	〃	90.6	91.4	92.2
Calculated Stokes' value							

Therefore the assumption of the critical size (1st approximation) is also proved to be adequate for calculation of collection efficiency.

The comparison of the calculated value and the measured efficiency shown in Fig 4.6 proves that the calculated formula is approximately correct.

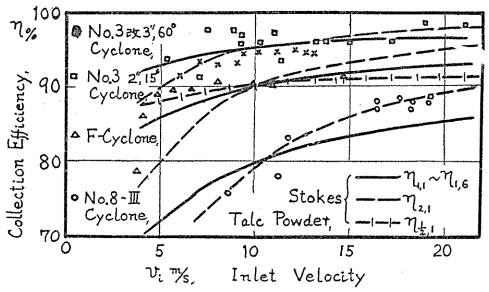

FIG. 4.6. Effect of inlet velocity.

B. Effect of Cyclone Size m

If a cyclone changes its size m times proportionally, we have $\delta \propto \sqrt{m}$ (Stokes) or $\delta \propto m^{2/3}$ (Allen).

$\therefore$ 1st approximation

$$\eta_{n,1,m} = e^{-b(\sqrt{m}\delta)^n}, \quad \text{or} \quad \log \eta_{n,1,m} \propto m^{n/2}, \qquad \text{(Stokes)}$$

$$\log \eta_{n,1,m} \propto m^{2n/3}, \qquad \text{(Allen)}$$

Other approximate formulae are similar to those in the previous section. The comparison between the calculated value and the measured efficiency is given in Table 4.2.

TABLE 4.2. Effect of the Cyclone Size on the Efficiency.

Cyclone No.	No. 5	No. 4	No. 6	D	No. 8-I
Cyl. Dia. D cmϕ	14.5	28.4	125.0	30	55
Measured Eff.	98	96	—	94	85(89)
$\eta_{1,1,m}$	97	〃	89	〃	92
$\eta_{2,1,m}$	98	〃	84	〃	89

Note: Measured value is about the maximum efficiency. Talc powder is used.

C. Effect of Diameter of Exit Pipe $d = 2r_e$

From the previous formula, we get; $\delta \propto r_e^{n'}$, where $n' = 0.5 \sim 1.5$ (Stokes) or $0.3 \sim 2.0$ (Allen), and from the 1st approximation;

$$\eta_{1,1,n'} = R = 10^{-b'' r_e^{n'}},$$

Table 4.3 gives several examples of experimental results, in which $n' = 1$ seems to be adequate.

TABLE 4.3. Effect of the Exit Radius of the Cyclone on the Efficiency.

Cyclone	No. 4		No. 8		No. 3			C type		E type	
r_2 (cm)	5.8	3.2	28.5	20.0	5.1	3.95	2.55	7.5	6.0	7.5	6.0
η_m (%)	94	(96)	(85)89	93	96	97～98	98～99	90	91	95	96
$\eta_{1,1,1}$ (%)	〃	96.6	〃	(89.1)92.2	〃	97.0	98.0	〃	92.0	〃	96.0
$\eta_{1,1,1/2}$ (%)	〃	95.5	〃	(87.2)90.7	〃	96.5	97.2	〃	91.0	〃	95.5

Note: Talc powder is used. η_m is measured Efficiency

D. Effect of Cylinder Length L

From the approximate formula of the pressure loss in the cyclone,

$$P_i \propto (L+H)^{1/2}, \quad \text{and} \quad P_i \propto v_0^2, \qquad \therefore\ v_0 \propto (L+H)^{-1/4},$$

where H is length of the conical part, and the inlet velocity v_i is constant. The radial velocity v_r is assumed to be unaffected by the cylinder length L.

$\therefore\ v_r = \text{const.}$

$$\delta \propto \frac{\sqrt{v_r}}{v_0} \propto \sqrt[4]{L+H}, \qquad \text{(Stokes)}$$

or

$$\delta \propto \frac{v_r}{v_0^{4/3}} \propto \sqrt[3]{L+H}, \qquad \text{(Allen)}$$

i.e. longer cylinder length gives larger critical separation size δ and lower efficiency η. 1st approximation;

$$\therefore\ \log \eta_{n,1} \propto (L+H)^{n/4}, \qquad \text{(Stokes)}$$

or

$$\log \eta_{n,1} \propto (L+H)^{n/3}, \qquad \text{(Allen)}$$

The experimental results of C, D and E types of cyclones shown in Table 4.4 indicate that the above formula is fit to them, and that a longer cylinder cyclone gives an efficiency 1～3% lower than a shorter one.

TABLE 4.4. Effect of Cylinder Length L (C, D and E type cyclone).

Cylinder Length	Collection Efficiency		Remark
$L=$ 32 cm	$\eta = 95\%$	92%	Based value
125 cm	94	90	Calculated value

E. Effect of Inlet Area a

Similarly to the previous paragraph,

$$P_i \propto a, \quad \text{and} \quad P_i \propto v_0^2, \qquad \therefore\ v_0 \propto \sqrt{a}$$

and,

$$v_r \propto Q = a v_i, \qquad \therefore\ v_r \propto a, \qquad (v_i = \text{const.})$$

then,

$$\delta \propto \sqrt{v_r}/v_0 \propto \sqrt{a}/\sqrt{a} = \text{const.}, \qquad \text{(Stokes)}$$

or

$$\delta \propto v_r/v_\theta^{4/3} \propto a/a^{2/3} = a^{1/3}, \qquad \text{(Allen)}$$

The first approximation gives the following formula at the same inlet velocity;

$$\log \eta_{n,1} \propto \text{const.}, \qquad \text{(Stokes)}$$

$$\log \eta_{n,1} \propto a^{n/3}, \qquad \text{(Allen)}$$

F. Effect of Cylinder Diameter D

$$P_i \propto \sqrt{D}, \quad \text{and} \quad P_i \propto v_\theta^2, \qquad v_\theta \propto \sqrt[4]{D},$$

and v_r is assumed not to be affected by cylinder diameter D,

$$\therefore\ \delta \propto \sqrt{v_r}/v_\theta \propto D^{-1/4}, \qquad \text{(Stokes)}$$

or

$$\delta \propto v_r/v_\theta^{4/3} \propto D^{-1/3}, \qquad \text{(Allen)}$$

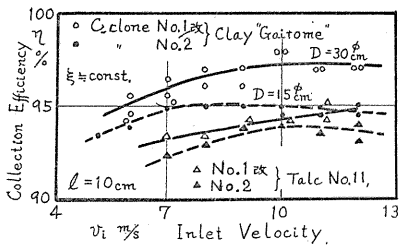

FIG. 4.7. Effect of cylinder diameter.

The first approximation becomes at the same inlet velocity as follows:

$$\log \eta_{n,1} \propto D^{-n/4} \qquad \text{(Stokes)}$$

or

$$\log \eta_{n,1} \propto D^{-n/3}, \qquad \text{(Allen)}$$

An experimental reault (Fig. 4.7) shows that the above formulae are correct on the whole.

G. Effect of Cone Angle ξ

Length H of conical part is related to the cone angle ξ by the following formula

$$H = (D - d')/(2\tan\xi/2),$$

where d' is diameter of dust port. From the approximate formula for pressure loss, we get $v_\theta \propto (L+H)^{-1/4}$, and assume that the radial velocity v_r would not be affected by the cone length H.

$$\delta \propto \sqrt{v_r}/v_\theta \propto (L+H)^{1/4}, \qquad \text{(Stokes)}$$

or

$$\delta \propto v_r/v_\theta^{4/3} \propto (L+H)^{1/3}, \qquad \text{(Allen)}$$

then,

$$\log \eta_{n,1} \propto (L+H)^{n/4}, \quad \text{(Stokes)} \quad \text{or} \quad (L+H)^{n/3}, \quad \text{(Allen)}$$

The larger the cone angle ξ becomes, or the shorter the cone length H grows, the better the efficiency becomes according to this assumption. But the effect of the cone angle is not simple, and has another action on the efficiency. The particle is thrown out on the conical wall by the centrifugal force, and is balanced by reaction of the wall and gravity (Fig. 4.8).

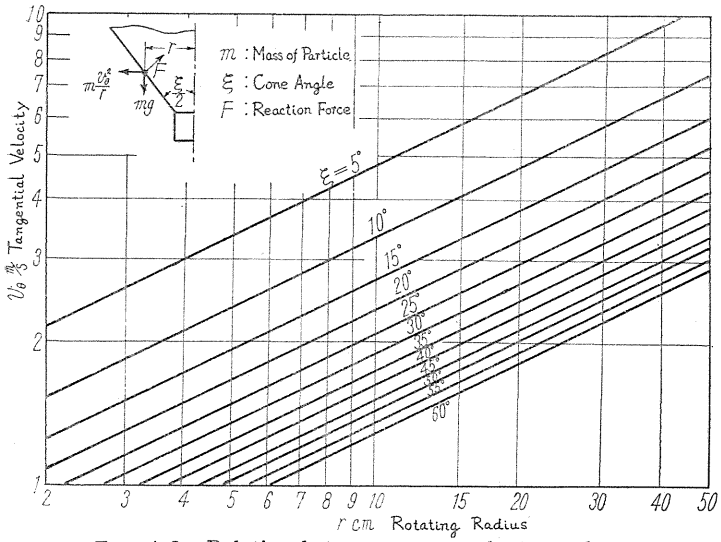

FIG. 4.8. Relation between cone angle (ξ) and balanced radius (r) and rotational velocity (v_θ).

$$mg\cos\tfrac{\xi}{2}/2 = m\frac{v_\theta^2}{r}\sin\tfrac{\xi}{2}/2,$$

$$\therefore\ \tan\tfrac{\xi}{2}/2 = rg/v_\theta^2,$$

This relation is shown in Fig. 4.6. When the cone angle is large enough, it is difficult to settle dust particles down into a dust chamber, and naturally the collection efficiency falls. This balanced radius r of rotation can be observed with a glass cyclone. In this case a longer cone is desirable in the contrary to the previous 1st approximation. Therefore, from the above two theories, the optimum cone angle exists at about 15°~30° for each cyclone under given testing or operating conditions. The experimental results are given in Table 4.7 and 4.8.

TABLE 4.7. Effect of Exit Diameter (d) and Cone Angle (ξ) on the Collection Efficiency in No. 3′ Cyclone, (L=155 mm)

I. Powder Clay "Gairome," Inserted Length of Exit Pipe l=10 cm.

a. Inlet Velocity v_i=12.5 m/s (Constant).

$d\downarrow$ $\xi\rightarrow$	15°		30°		60°	
2″ 51 φ (mm)	96.0(%) 96.0 96.5	(96.2) P_i=96	96.5(%) 96.5 96.5	(96.5) P_i=125	91.5(%) 91.5 91.5	(91.5) P_i=150
3″ 79 φ	95.5 94.5 95.5	(95.2) P_i=38	96.5 94.5 95.5	(95.5) P_i=47	95.0 95.5 95.5	(95.3) P_i=60
4″ 102 φ	92.5 93.5 93.5	(93.2) P_i=21	94.5 95.0 95.0	(94.8) P_i=28	93.0 93.5 93.0	(93.2) P_i=32

Note: ξ=Cone angle, d=Exit diameter, (η_m%)=Mean efficiency, P_i=Pressure loss,

TABLE 4.7. (*Continued*)

b. Pressure Drop P_i=34 mm Aq (Constant).

d↓ ξ→	15°		30°		60°	
51 ϕ (mm)	95.8(%)	(v_i=7.5)	**96.7**(%)	(6.7)	**96.8**(%)	(6.0)
79	93.5	(12.0)	94.8	(10.7)	**96.7**	(9.5)
102	92.7	(15.6)	95.2	(13.8)	93.3	(12.8)

Note: (v_i m/sec.)=Inlet velo., Efficiency is a mean value,

II. Powder Talc No. 11.

d↓ ξ→	15°		30°		60°		v_i (m/sec.)
51 ϕ(mm)	95.3(%)	l= 0(cm)	**96.5**(%)	l=10(cm)	71.5	l=20(cm)	12.3~12.9
79	95.8	l=10	95.5	l=20	91.0	l= 0	13.8~15.1
102	93.2	l=20	84.0	l= 0	91.5	l=10	15.0~15.6

Note: l=Inserted length of exit pipe, v_i=Inlet velocity, Efficiency is a mean value of three measured eff.,

TABLE 4.8. Effect of Exit Diameter (d) and Cone Angle (ξ) on the Collection Efficiency in No. 3 Cyclone (L=540 cm).

d↓ ξ→	15°	30°	60°
51 ϕ (mm)	**98.5**(%)	98.3	97.5
79	97.4	98.2	96.9
102	92.6	95.7	96.1

Note: Powder=Talc No. 3, 4, Inserted length of exit pipe l=7 cm, Inlet velocity $v_i \fallingdotseq 20$ m/s, Efficiency is a mean value,

But it must be also noticed that higher tangential velocity in a cyclone may grind and disperse the powder, and may decrease the efficiency.

H. Effect of the Kind of Powder

By the first approximation

$$\eta_{n,1} = R = 10^{-b'\delta n}, \quad \text{and} \quad \delta_y = \sqrt{\rho_{sx}/\rho_{sy}}\cdot\delta_x, \qquad \text{(Stokes)}$$

or

$$\delta_y = (\rho_{sx}/\rho_{sy})^{2/3}\delta_x, \qquad \text{(Allen)}$$

$$\therefore \quad \frac{\log \eta_{n,1,y}}{\log \eta_{n,1,x}} = \frac{b'_y}{b'_x}\left(\frac{\rho_{sx}}{\rho_{sy}}\right)^{ny/2}\delta_x^{ny-nx}, \qquad \text{(Stokes)}$$

or

$$\frac{\log \eta_{n,1,y}}{\log \eta_{n,1,x}} = \frac{b'_y}{b'_x}\left(\frac{\rho_{sx}}{\rho_{sy}}\right)^{2ny/3}\delta_x^{ny-nx}, \qquad \text{(Allen)}$$

Experimental results of talc and dolomite powder are shown in Table 4.5, and this approximate formula gives the likely values.

TABLE 4.5. Effect of Difference between Talc and Dolomite Powder.

Cyclone	No. 4		No. 5			No. 2	Remark
Inlet Velo. v_i	7	10	6.0	8.3	10.5	16	m/sec
η_x (Talc)	0.90	0.95	0.80	0.90	0.96	0.94	
η_y (Dolomite)	0.83	0.86	0.62	0.79	0.90	0.85	
$\log \eta_y / \log \eta_x$	1.8	2.9	2.1	2.2	2.6	2.6	Experiment
Right Side	1.6	2.2	1.2	1.6	2.1	2.1	Stokes

6. Discussion of Other Formulae

The formulae by other investigators (Rosin, Rammler and Intelman,[13] Linden,[14] Watanabe and Kawabata,[26] Ikemori,[25] Kitaura,[28] etc.) are unfit for the practical use, because they contain many unreasonable and indefinite assumptions, and give too large critical diameter of powder particles for separation to estimate the collection efficiency.

4. Experimental Results

I have experimented on collection efficiencies of various types of cyclones, and discussed these results with my theory. The main results are as follows:

A. Error of Measured Collection Efficiency

When supplied amount of powder is little, the percentage of clinged amount is rather considerable. And the size distribution of the powder is not strictly constant. Therefore comparative error of the efficiency happens. When the size of cyclone is large, the supplied amount of powder must be increased. Table 4.6 shows the error of efficiency in relation to the supplied amount of powder.

TABLE 4.6. Error of the Efficiency against Supplied Amount.

Supplied amount	Measured collection efficiency	Mean value	Standard deviation	Reliable limit of mean value (5%)
100 g	84.0, 76.5, 80.3, 76.8, 78.5, 78.0, 79.9,	79.1	2.57	76.8~81.5
200	81.2, 80.9, 80.9, 77.4, 80.2, 81.8, 78.7,	80.2	1.56	78.7~81.7
400	82.9, 84.0, 82.9,	83.3	0.64	81.7~84.9

Note: Talc powder and No. 8-I type cyclone are used.

B. Effect of Inlet Velocity v_i

Inlet velocity has an optimum value at about 10~15 m/s, but when cone angle or inlet area is large, or when exit diameter is small, a lower inlet velocity gives the maximum efficiency (Fig. 4. 9). This fact is explained in the paragraph of cone angle. And the lowest velocity gave the maximum efficiency in a particular case.

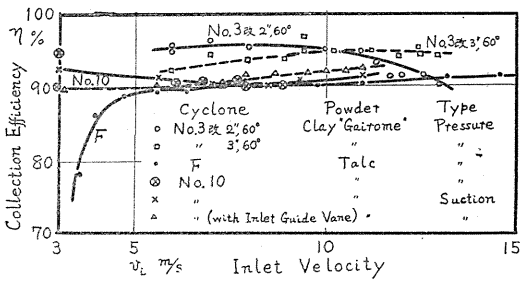

FIG. 4. 9. Effect of inlet velocity.

C. Effect of Closing and Opening of Dust Port

Dust box of the suction type must be shut air-tight, and that of the delivery (pressure) type should be rather shut usually (Fig. 4.10). This is due to suction flow from the dust port.

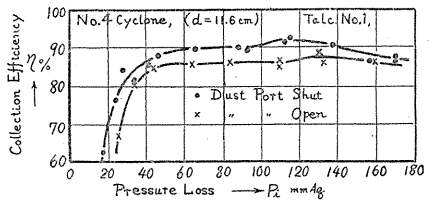

FIG. 4.10. Effect of closing or opening of dust port.

As supplied rate of powder is larger, the decrease of the efficiency becomes smaller.

D. Effect of Inserted Pieces

Inserted pieces such as inlet or central guide vane or horizontal disc were not good on the whole, but they had often good characteristics under the special condition. The horizontal disc in dust box of a cylindrical cyclone (No. 9 b) was effective (Fig. 4.11).

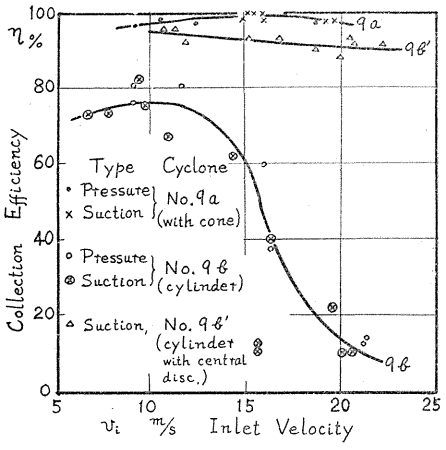

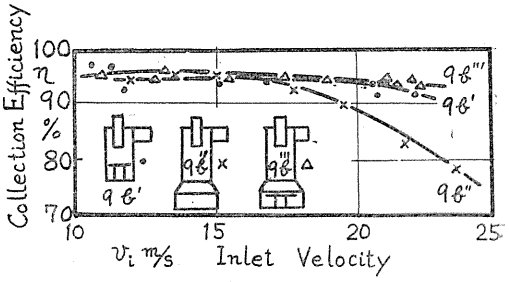

FIG. 4. 11 *a* (*left*). Effect of horizontal disc in the bottom.

FIG. 4 11 *b* (*right*). Effect of horizontal disc in the bottom.

E. Effect of Form of Inlet Part

There are many forms of inlet part such as tangential, semispiral and full spiral type, but the difference of these forms had little effect on the characteristics of the cyclone. The section of inlet port, of which longitudinal length is longer than the traverse length, was desirable. And it was undesirable that an inlet pipe is arranged in such a way as its elongation crosses the exit pipe. However in the latter case an inlet guide vane or an upward inclined inlet pipe (about 10°) improved the characteristics (No. 10 Cyclone).

F. Effect of Feeding Position

The feeding position of test powder and the position of cyclone against a blower (delivery or suction side) were not important. Outer feed of powder in the inlet pipe did not give better efficiency than inner feed. Therefore Rosin's theory about collection efficiency is not adequate. And the regulating position of gas quantity was not also important (No. 4 and No. 8 Cyclone).

G. Effect of Dust Concentration

As dust concentration increases, hindered settling and cohesion of powder particles take place, and wall friction becomes large. Therefore the collection efficiency might be affected by dust concentration, but its effect is shown to be negligible by the experiment (Fig. 4.12).

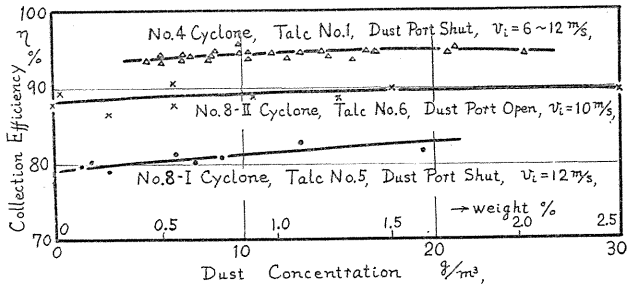

FIG. 4.12. Effect of dust concentration.

H. Horizontal Type

The horizontal cyclone, which is recommended by Mr. Linden, was not favourable, but it had a lower pressure loss (No. 4 Cyclone).

I. Effect of Inserted Length of Exit Pipe l

When the exit pipe is inserted a little deeper than the lower side of the inlet pipe, its efficiency is usually maximum. But at higher inlet velocity it is not necessarily the case in No. 8-I cyclone, the effect being so delicate (Fig. 4.13).

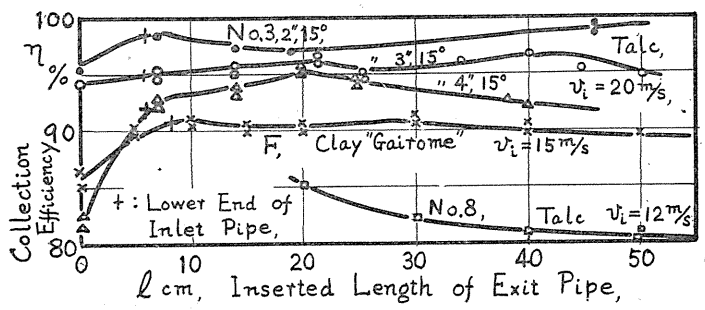

FIG. 4.13. Effect of inserted length of exit pipe.

J. Effect of Inner Friction

Inner friction is undesirable, and the efficiency is almost proportional to the pressure loss of a cyclone. Experiments of No. 2 cyclone showed that large wall friction (about 0.5~1 mm sand particle pasted) reduced collection efficiency, by several percent.

K. Effect of Powder

Size distribution of powder by the sedimentation method does not often coincide with that by the air elutriation method. The cyclone points on a size distribution figure, which were obtained from the measured collection efficiencies η_m, the approximate calculation ($\eta_m = R$) and assumed cut size of powder particle being used,

were shown along or slightly below (coarser than) the air elutriation curve. Namely the effects of various kinds of powder had good correlation with the size distribution of the powder particle by the air elutriation method. But the specific surface area did not always give good correlation with the collection efficiency.

5. Conclusion

The author tried to derive a theory of collection efficiency in a cyclone, and experimented on various types of cyclones. My approximate formulae were applicable to the experimental results with good agreement on the whole, and either of Stokes' or Allen's law can be used for the sedimentation of powder particle in a cyclone.

The effects of opening and closing of dust port, inserted pieces, form of inlet part, diameter and inserted length of exit pipe, inlet velocity, cone angle, diameter and length of cylindrical part, inner wall friction, feeding position of powder, regulating position of gas quantity, pressure and suction type, dust concentration, size distribution of powder etc. were examined on many cyclones under various conditions, and the results were discussed.

Chapter V. Characteristics of Some Special Types of Cyclones

1. Prelimimaries

The author made some special cyclones which were considered to be of improved types, and compared their characteristics with those of an usual cyclone through many experiments in cooperation with Mr. R. Toyoda. And he was indebted to the Nagoya Factory of Nisshin Flour-Mill Co. for aid in constructing and erecting the apparatus.

2. Test Cyclone

A. Van Tongeren Type (No. 8-VI)[12] (Fig. 5.1)

This type is an amended No. 8-I cyclone, which has a bypass from the top of cylindrical part to conical part of the cyclone.

B. Parent and Child Type (No. 8-VII) (Fig. 5.2)

This type has one or two small cyclones around the exit pipe of No. 8-I cyclone.

C. Helical Top Type (B-Type) (Fig. 5.3)

This cyclone has a helical top deck,[22] and its mean spiral angle is about 10°, being similar to the spiral angle of the air flow. The dust chamber has a blow down pipe.[34]

D. Circular Inlet Guide Vane Lattice Type (C-Type) (Fig. 5.4)

This cyclone has a spiral inlet and six guide vanes on the periphery, intended to obtain uniform inlet flow.

E. Tangential Inlet Normal Type (D-Type) (Fig. 5.5)

This is similar to No. 8-I cyclone reduced in size, and is of standard type.

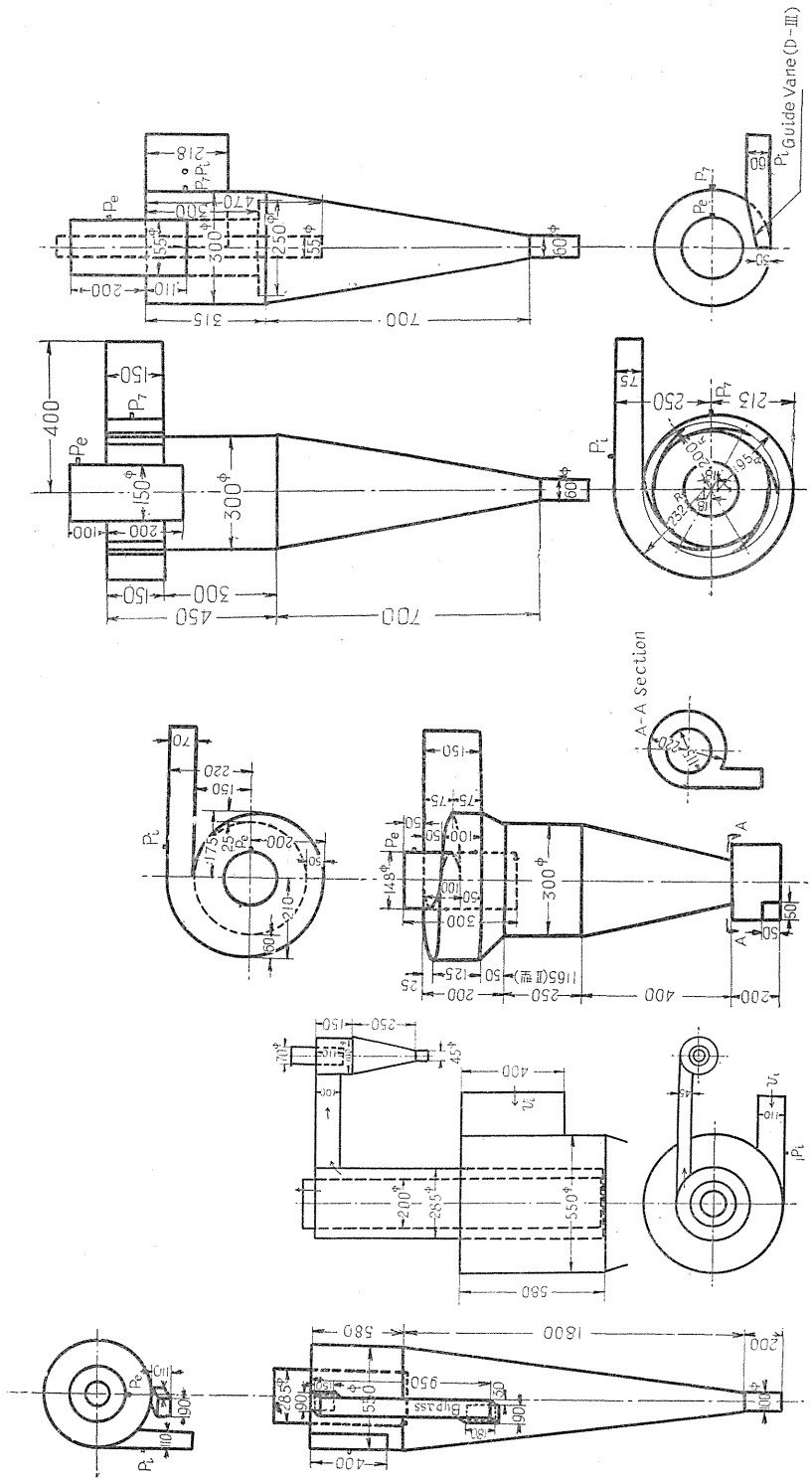

FIG. 5.1. Van tongeren type (No. 8-VI). FIG. 5.2. Parent and child type (No. 8-VII). FIG. 5.3. Helical top type (B-Type).
FIG. 5.4. Circular inlet guide vane lattice type (C-Type). [E-type is without the vane lattice.] FIG. 5.5. Tangential inlet normal type (D-Type) (with a central small cylinder or an exit end flange).

which has simple construction. A central small cyinder or a lower-end flange of the exit pipe, and also an inlet convergent guide vane (D-III type) can be attached to the cyclone.

F. Circular Inlet Space Type (E-Type) (Fig 4.5)

This type has a spiral inlet and an annular inlet space on the periphery of the cylindrical top, and it is simpler than C-type without the vane lattice.

In general, the type "II" has longer cylindrical part than the type "I," and the type "a" has larger exit pipe diameter than the type "b."

3. Experimental Results

A. No. 8-VI Cyclone (Van-Tongeren Type)

This type had a little lower pressure loss than No. 8-I (standard) cyclone, and gave almost as good collection efficiency. The experiments showed that this was not effective.

Spiral exit is ineffective and innocuous, and larger diameter of dust port is not advantageous (Fig. 5.6).

B. No. 8-VII Cyclone (Parent and Child Type)

This type had not any better collection efficiency either, because the amount of collected dust by the small cyclone was little.

This cyclone showed very lower efficiency by attaching a divergent inlet guide vane, and the relation between No. 8-II and No. 8-V cyclones was just the same, the latter with a divergent inlet guide vane showing poor efficiency. (Fig. 5.7)

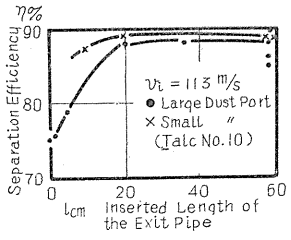

FIG. 5.6 (*left*). Effect of diameter of the dust port (No. 8-VI Cyclone).

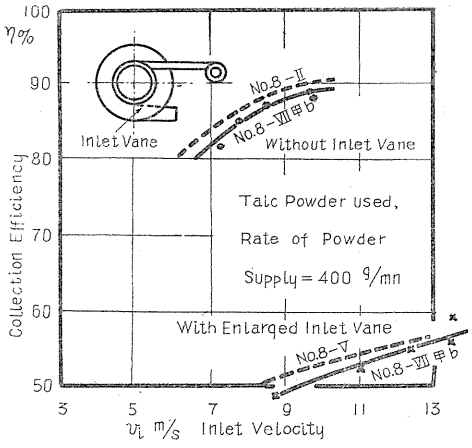

FIG. 5.7 (*right*). Characteristics of No. 8-VII 甲 b type cyclone.

C. B-Type (Helical Top Type)

This type had lower pressure loss but lower collection efficiency contrary to expectation (Fig. 5.8). The longer cylinder type (II) gave unusually higher efficiency than the shorter cylinder one (I).

Effect of inserted length of exit pipe was sensitive and delicate in efficiency, but the maximum efficiency occured, when the insertion extended slightly lower than the lower side of the inlet pipe (Fig. 5.9). Blowing down of the dust box

was found not to be much effective in this case. The flow pattern of the cyclone is given in Fig. 5.10, and we can study many matters from this pattern.

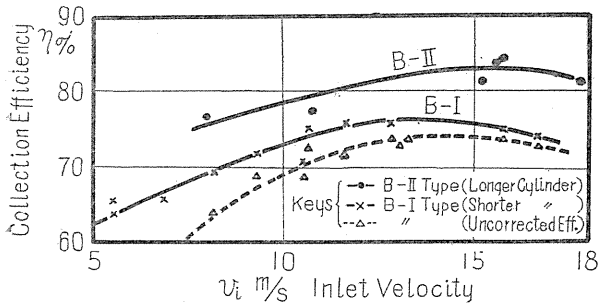

FIG. 5.8. Collection efficiency of B type cyclone.

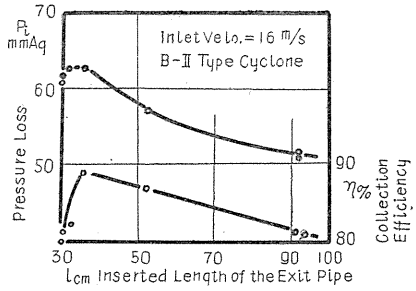

FIG. 5.9. Effects of inserted length of the exit pipe (B-II Type Cyclone).

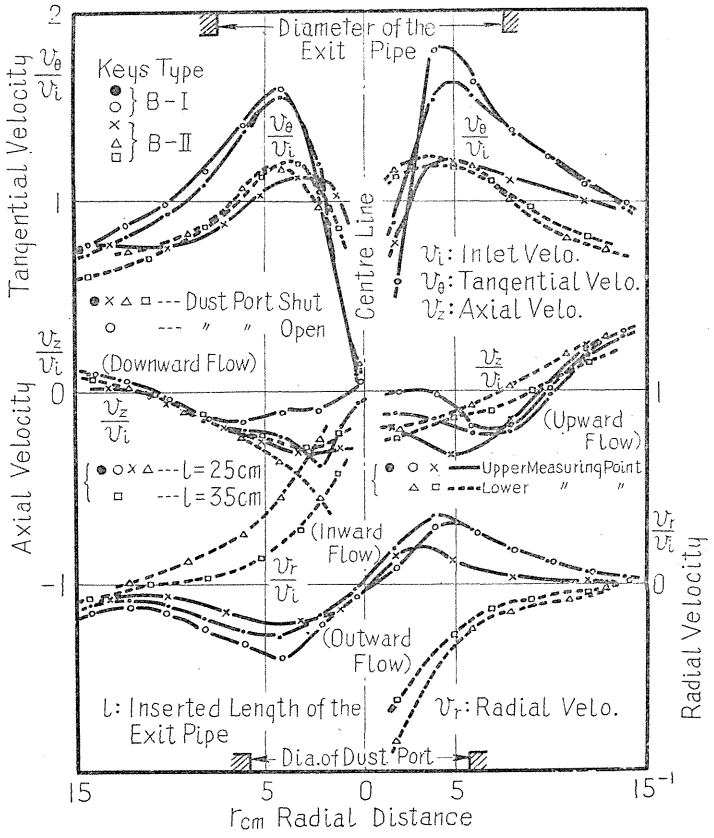

FIG. 5.10. Flow distributions of B type cyclone (measured by a spherical Pitot tube).

D. C-Type (Annular Inlet Guide Vane Lattice Type)

This cyclone had complicated construction but good characteristics, such as lower pressure loss and fairly good efficiency.

The longer cylinder type (II) had lower pressure loss and lower efficiency than the shorter one (I), and the smaller exit type (b) had higher loss and higher efficiency than the larger one (a). This type showed also delicate effect of the inserted length of exit pipe.

E. D-Type Cyclone (Normal Tangential Inlet Type)

This type had simple construction, higher efficiency but the highest pressure loss.

The convergent inlet guide vane type (D-III), as the other types, gave lower pressure loss and lower efficiency.

When a solid central small cylinder was inserted, the efficiency decreased slightly. But a hollow central small cylinder was a little promising (Fig. 5.5).

A flange posted at the lower end of the exit pipe, aiming to keep the secondary flow away from the entrance of the exit pipe, was found not to be effective.

F. E-Type Cyclone (Annular Inlet Space Type)

This type had higher pressure loss but the highest collection efficiency.

A Shorter cylinder gave higher efficiency than a longer one, and a small hollow cylinder inserted at the center of the cyclone, was promising.

4. Conclusion

In general, the normal tangential inlet type (D) and the annular inlet space type (E) are desirable, and longer length of the cylindrical part reduces pressure loss fairly and also collection efficiency slightly (C, D, E).

If the diameter of exit pipe is too small, it causes only higher pressure loss, and improves scarcely collection efficiency (Table 5.1 and Table 5.2).

Inserted length of the exit pipe has delicate effect on both pressure loss and collection efficiency, and any of the devices, such as inlet vane, flange, larger dust port, spiral exit or central small pipe, was found not to be much effective. With these results, the theory of a cyclone was proved to be approximately correct, and reference data for design of cyclones were obtained.

TABLE 5.1. Effects on the Collection Efficiency by Cylinder Lengths and Exit Diameters of Cyclones.

Type	Dia. of Exit (cm)	I. Shorter cylinder (L=32 cm)		II. Longer cylinder (L=125 cm)		Remarks
		Measuring efficiency	Mean	Measuring efficiency	Mean	
B	14.8		78 %		81~84%	Helical top
C-a	15	93.5, 92.5, 92.0	92.7	88.5, 90.0, 90.5	89.7	With inlet vane lattice
C-b	12	91.0, 93.0, 93.0	92.3	89.5, 92.5, 91.5	91.2	
D	15.5	94, 94, 94	94.0	92, 93, 90	91.7	Tangential inlet
E-a	15	94, 96	95.0	93.5, 94.0	93.8	With inlet annular space
E-b	12	96, 96	96.0	94, 96	95.0	

Notice: Talc powder used, Measuring efficiencies are the maximum values at inlet velo. v_i=10~15 m/s, and at pressure loss P_i=60~140 mm Aq.

TABLE 5.2. Characteristics of Special Type Cyclones.

Type	Coeff. of press. loss F	n $(P_i \propto V_i^n)$	Max. eff. η_{max} (%)	Cyl. dia. D ϕ (cm)	Inlet area a (cm²)	Exit. dia. d ϕ (cm)	Total length $(L+H)$ (cm)	Remarks
No. 8-I	10	2.0	85(89)	55	440	28.5	238	Tangential inlet normal
No. 8-VI甲	7.9	2.2	90	〃	〃	〃	〃	Van tongeren with scoop
No. 8-VI乙	8.6	2.1	84(92)	〃	〃	〃	〃	〃 without scoop
No. 8-VIIα	10.6	1.8	85-	〃	〃	〃	〃	With a small cyclone
No. 8-VIIβ	19	2.4	89-	〃	〃	20.0	〃	〃 (Double exit)
B-I	4.4	2 0	78	30	105	14.8	85	Helical top
B-II	3.4	2 1	81(84)	〃	〃	〃	177	Helical top
C-I-a	5.6	2.1	93	〃	131	15	115	With inlet guide vane lattice
C-I-b	8.3	2.2	92	〃	〃	12	〃	With inlet guide vane lattice
C-II-a	4.8	2.1	90	〃	〃	15	207	With inlet guide vane lattice
C-II-b	6.4	2.1	91	〃	〃	12	〃	With inlet guide vane lattice
D-I	14.6	2.3	94	〃	〃	15.5	102	Tangential Inlet
D-II	8.7	2.2	92	〃	〃	〃	194	〃
D-III	12.7	(3.0)	90	〃	131×½	〃	102	〃 (with inlet vane)
E-I-a	10.7	2.3	95	〃	113	15	115	With inlet annular space
E-I-b	16.2	2.1	96	〃	〃	12	〃	With inlet annular space
E-II-a	8.1	2.2	94	〃	〃	15	207	With inlet annular space
E-II-b	10.7	2.1	95	〃	〃	12	〃	With inlet annular space

Notice: $F=P_i/\frac{1}{2}\rho v_i^2$ is at $v_i \fallingdotseq 10$ m/s., η_{max}. is the Maximum collection efficiency, which is tested by talc powder.

Summary

The optimum inlet velocity (about 10~15 m/s) should be used in practice, and the blower must have over 200 mm Aq. static pressure.

A favourable type of the cyclone is such as E or D type in Chapter V, and smaller size of the cyclone has better collection efficiency, but it can deal with only a small quantity of gas. Any of the various devices is not effective generally except in the special case.

A favourable proportion of the cyclone is commonly as follows:

$$\sqrt{a} \fallingdotseq 0.35\ D,\ L \fallingdotseq D,\ d \leqq D/2,\ \xi = 20° \sim 30°,\ d' \fallingdotseq d/2,$$

where D is diameter of the cyclone, a is inlet area, L is height of the cylindrical part, d is diameter of the exit pipe, ξ is cone angle, and d' is diameter of the dust port.

Pressure drop and collection efficiency of an arbitrary cyclone can be calculated for a given condition by my theory.

If it is desired to reduce the pressure loss of the cyclone, its length should be elongated, or some obstacles should be inserted into the cyclone.

The dust port must be closed air-tightly.

For regulation of air flow quantity, it is not adequate to use a throttle valve, but it should be appropriate to change the blower speed, or to stop work of some units of multi-cyclones.

Acknowledgement

The author is grateful to Hydraulic Laboratory, Department of Mechanical Engineering, Nagoya University for the use of laboratory equipment and facilities, to Prof. Dr. K. Shogenji and Prof. Dr. K. Kaneshige for their guidances and encour-

agements, to Mr. N. Kimura and some students for their earnest assistances, and to several Companies for aid in constructing the apparatus. And this research is partially indebted to the fund of scientific research of the Educational Department of Japan.

References

1) Shogenji and Shimoyama: Memoirs of the Faculty of Engineering, Kyushu Imperial University, **7**, 3, (1933); and J.J.S.M.E. **35**, 181, (1932–5), p.422.
2) Kaneshige: Memoirs of the Faculty of Engineering, Tokyo Imperial University, **17**, 8, (1928-4).
3) Iinoya: Research Reports of The Faculty of Engineering, Nagoya University, **III-1**, (1950), p. 5, and **III-2**, (1950), p. 95.
4) Lamb: Hydrodynamics, (1952), p. 577.
5) Goldstein: Modern Developments in Fluid Dynamics, **I**, (1938), p. 315.
6) Whiton: Power, **75**, (1932-3), p. 344, and Chem. and Met. Engg., **39**, (1932-3), p. 150.
7) Feifel: Archiv für Wärmewirtschaft und Dampfkesselwesen, **20**, 1, (1939-1), p. 15, and Forschung, **9**, 2, (1938-3, 4), p. 68, and **10**, 5, (1939-9, 10), p. 212.
8) Schepherd and Lapple: I.E.C., **31**, 8, (1939-8), p. 972,: **32**, 9, (1940-9), p. 1246.
9) Alden: Heating and Ventilating, **35**, 7, (1938-7), p. 48.
10) First and Silvermann: Heating and Ventilating, **45**, 7, (1948-7), p. 80.
11) Lissman: Chem. and Met. Engg., **37**, (1930), p. 630.
12) Tongeren: Mech. Engg., **57**, 12, (1935-12), p. 753.
13) Rosin, Rammler and Intelmann: Z.V.D.I., **76**, 18, (1932-3), p. 433.
14) Linden: Engg., **167**, 4334, (1949-2-18), p. 165, and P.I.M.E., **160**, 2, (1949), p. 233.
15) Schneider: C. E. Review, **53**, 2, (1950-2), p. 22.
16) Monroe: Heating and Ventilating, **47**, 12, (1950-12), p. 63.
17) Stairmand: Engg., (1949-10-21), p. 409.
18) Perry: Chem. Engr's Handbook, (1950), p. 1023.
19) Taggert: Elements of Ore Dressing, (1950), p. 110.
20) Taggert: Handbook of Ore Dressing, (1950), p. 9–07.
21) Lapple: Chem. Engg., (1951-5), p.144.
22) Hopf: Mühlentechnisches Praktikum, **1**, p. 424, and **2**, p. 240.
23) Silvermann: Heating and Ventilating, **50**, 2, (1953-2), p. 87.
24) Lapple and Dietrich: Chemie Ing. Tech., **25**, 4, (1953-4), p. 185.
25) Ikemori: T.J.S.M.E., **8**, 33, (1942), p. 68, 72 and 74, and **15**, 50, (1949), p. 57.
26) Watanabe and Kawabata: Chem. Engg., (Japan) **14**, 3, (1950), p. 116, and Seisan Gijutsu, **4**, 5, (1952-5) p. 14.
27) Urabe: Tetsudo Gyomu Kenkyu Shiryo, 8, 13, (1951), p. 5, and Tetsudogiken Dooryokusha Kenkyushitsu Report, **37**, (1950-7).
28) Kitaura: Chem. Engg, (Japan) **15**, 5, (1951), p. 206, and **16**, 8, (1952), p. 249, and p. 254.
29) Asao: Hitachi Shipbuilding Tech. Report, **11**, 4, (1950), p. 3, and **13**, 2, (1952), p. 16.
30) Ikemori and Makita: Nichidai Kogakubu Kenkyujo Iho, **4**, (1952-4), p. 23.
31) Nishihara and Kori: T.J.S.M.E., **18**, 69, (1952), p. 48.
32) Murakami and Fukunaga: T.J.S.M.E., **18**, 73, (1952), p. 56.
33) Ikemori: J.J.S.M.E., **55**, 404, (1952-9), p. 14.
34) Power, **95**, **6**, (1951-6), p. 104.
35) Iinoya: T.J.S.M.E., **18**, 66, (1952), p. 90, (1st Report); 18, 69, (1952), p. 42, (2nd Report); **19**, 81, (1953), p. 78, (3rd Report); p. 83, (4th Report), p. 90, (5th Report) and **20**, 89, (1954), p. 38, (6th Report).
36) Iinoya: Chem. Engg., (Japan) **16**, 8, (1952-8), p. 261; **17**, 5, (1953-5), p. 185 and **18**, 4, (1954-4).